

Tangles: From Weak to Strong Clustering

Christian Elbracht*¹ Diego Fioravanti*³ Solveig Klepper*² Jakob Kneip*¹
Luca Rendsburg*² Maximilian Teegen*¹ Ulrike von Luxburg^{2,3}

¹Department of Mathematics, University of Hamburg, Germany

²Department of Computer Science, University of Tübingen, Germany

³Max-Planck-Institute for Intelligent Systems, Tübingen, Germany

{christian.elbracht, jakob.kneip, maximilian.teegen}@uni-hamburg.de

dfioravanti@tue.mpg.de, solveig.klepper@student.uni-tuebingen.de

{luca.rendsborg, ulrike.luxburg}@uni-tuebingen.de

June 26, 2020

ABSTRACT

We introduce a new approach to clustering by using tangles, a tool that originates in mathematical graph theory. Given a collection of “weak partitions” of a data set, tangles provide a framework to aggregate these weak partitions such that they “point in the direction of a cluster”. As a result, a cluster is softly characterized by a set of consistent pointers. This mechanism provides a highly flexible way of solving soft clustering problems in a variety of setups, ranging from questionnaires over community detection in graphs to clustering points in metric spaces. Conceptually, tangles have many intriguing properties: (1) Similar to boosting, which combines many weak classifiers to a strong classifier, tangles provide a formal way to combine many weak partitions to obtain few strong clusters. (2) In terms of computational complexity, tangles allow us to use simple, fast algorithms to produce the weak partitions. The complexity of identifying the strong partitions is dominated by the number of weak partitions, not the number of data points, leading to an interesting trade-off between the two. (3) If the weak partitions are interpretable, so are the strong partitions induced by the tangles, resulting in one of the rare algorithms to produce interpretable clusters. (4) The output of tangles is of a hierarchical nature, inducing the notion of a soft dendrogram that can be helpful in data visualization.

1 Introduction

In this paper we present to the machine learning community a new tool that can be used for clustering: *tangles*. Tangles are an established concept in mathematical graph theory. They were originally introduced by Robertson and Seymour (1991) as a tool to study highly cohesive structures in graphs, and have since become a common tool in the analysis of other discrete structures (Diestel, 2018). Recently, the math community started to investigate applications of tangles, for example in the social sciences (Diestel, 2019).

To introduce the concept of tangles, we consider the example of a personality traits questionnaire, in which a group of persons answers a set of yes-no questions. Based on the answers, we would like to identify groups of like-minded persons and characterize their associated mindsets, such as being extroverted or introverted. One would expect that most persons who share a mindset agree on answers to relevant questions; for example, most introverts would answer “yes” to the question “Do you prefer to spend your free time alone?”. Accordingly, we would like to characterize a mindset by a soft way of saying that most persons with this mindset answer similarly to most questions. Tangles formalize this idea. First, we interpret every question as a partition of the persons into the ones answering “yes” and the ones answering “no”. We expect that most persons who share a mindset answer similarly, thus lie on the same side of such a partition. By identifying this side we can therefore orient the question to “point towards the mindset”. If a mindset is already known, we can orient every question in this way to characterize it as a “typical” way of answering. But since the task is to find the mindsets, we need to identify the meaningful orientations, which is precisely the purpose of tangles: a tangle is a consistent orientation of the partitions, where the consistency condition ensures that an orientation points

*Equal contribution.

towards a single structure (Figure 1). Typically, there exist multiple tangles on a given set of questions, and each of them corresponds to one mindset.

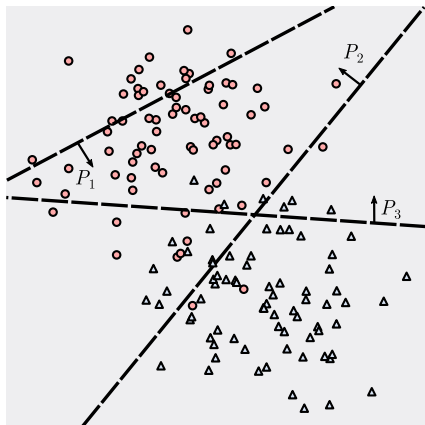


Figure 1: A tangle given by three consistently oriented partitions, pointing towards the ground-truth cluster given by the circles. The arrow at each partition P_i indicates the side towards which it is oriented. Changing the orientations of P_2 and P_3 yields another tangle that points towards the ground-truth cluster given by the triangles.

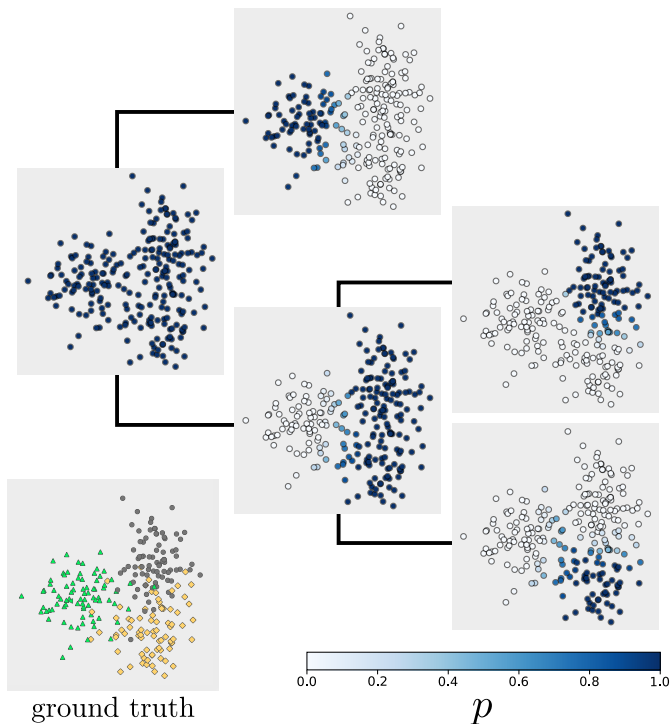


Figure 2: A soft dendrogram as possible post-processing of tangles (Supplement D.2). The probability that a point belongs to the respective node is given by p .

Benefits of tangles. Clustering with tangles offers a multitude of benefits. The **indirect characterization of a cluster by a set of pointers** does not rely on assigning cluster memberships to individual objects, which mitigates the problem of dealing with outliers and borderline cases. However, tangles can still be post-processed in various ways to generate hard clusterings, soft clusterings, or even soft dendrograms for hierarchical clustering, see Figure 2 for an example. Since the construction of tangles only requires a set of partitions of the data set as input, they can be employed in a large variety of settings.

On a high level, the tangle approach to clustering **resembles boosting** for classification. For the latter, one aggregates many weak classifiers, which are merely better than chance, to obtain a strong classifier. Tangles aggregate many weak clusterings (bipartitions) that contain the majority of some cluster on one of their sides to form a holistic view on the structure of a data set.

By focusing on bipartitions, tangles shift the attention in **computational complexity** from the number of objects to the number of bipartitions, which can be beneficial for large data sets. If the weak bipartitions come with an interpretation, so do the tangles: for example in the questionnaire setting, the partitions are given by the questions themselves. Tangles then reveal how persons with the same mindset typically answer the questions. This opens the door to **interpretable clustering algorithms**, as they might become more and more important when it comes to applying machine learning techniques in societal contexts.

Outline and contributions. In Section 2, we translate the abstract notion of tangles from the mathematical literature to a more practical version for machine learning. We then prove in Section 3 that tangles are able to discover the ground truth clusters in two typical scenarios: a statistical model for finding mindsets in the questionnaire setting, and the expected graph of the stochastic block model for graph clustering. In Section 4, we outline the algorithmic approach to discover tangles and discuss its application to various data sets and possible post-processing steps. An extensive set of experiments can be found in Section 5 and the supplementary material.

We consider this paper to be a first step and proof of concept for what we believe is a promising new direction of research in the field of clustering. There are ample opportunities for follow-up work regarding improved design of algorithms or extended theoretical results.

2 Tangles

We now formally introduce the framework of tangles.¹ As a running example to motivate the formal definitions, we use the questionnaire setting of the introduction (in colored font in parentheses).

2.1 Notation and definitions

Consider a set $V = \{v_1 \dots, v_n\}$ of arbitrary objects (the set of persons that took the questionnaire) whose cohesive substructures we would like to discover (persons that share the same mindset). We will use the notation $A \subseteq V$ for a subset of the objects, and A^c for its complement. A cut or bipartition of V consists of a set $A \subseteq V$ and its complement, denoted by $\{A, A^c\}$ (for example, the persons that answer “yes” to the first question and the persons that answer “no”). We consider a set of initial cuts $\mathcal{P} = \{\{A_1, A_1^c\}, \dots, \{A_m, A_m^c\}\}$ (the partitions induced by all the questions). Generally, the cuts in \mathcal{P} might separate substructures of V to different levels of granularity, and some cuts might not be informative at all. To judge on an abstract level how useful a cut might be, we introduce a cost function $c: \mathcal{P} \rightarrow \mathbb{R}_{\geq 0}$ for cuts. One natural way to do so is to assume that there exists a similarity function $\text{sim}: V \times V \rightarrow \mathbb{R}$ that judges how similar individual objects are (for example, we judge the similarity of two persons by counting how many questions they have answered the same way). We then define the cost of a cut $\{A, A^c\}$ as $\sum_{v \in A, w \in A^c} \text{sim}(v, w)$. In a graph setting, this cost coincides with the cut value of a graph cut. Note that this is just one way to define a cost function; depending on the application other cost functions can be chosen as well. By restricting the set of initial cuts to $\mathcal{P}_\Psi = \{P \in \mathcal{P} \mid c(P) \leq \Psi\}$ for some $\Psi \in \mathbb{R}_{\geq 0}$, we exclude cuts that separate highly connected structures. Controlling the parameter Ψ enables us to discover a whole hierarchy of substructures: for small Ψ , we can only distinguish between coarse structures (such as extroverts and introverts), while for large Ψ , we include cuts that further separate them into more fine-grained structures. After fixing Ψ , we need to find an orientation of the cuts in \mathcal{P}_Ψ that “points towards a cluster” (to find a set of persons with the same mindset, we will identify a typical way to answer the questions). Formally, an *orientation of a cut* $\{A, A^c\}$ simply selects one of its sides, A or A^c , and an *orientation O of \mathcal{P}_Ψ* is a set consisting of exactly one orientation for each cut $\{A, A^c\} \in \mathcal{P}_\Psi$. (An orientation of the questions is one way of answering the questionnaire.) Our intuition is that clusters can be characterized by orientations, but not every orientation characterizes a cluster (the answers to the questions need to be consistent in some way). Thus, we have to ensure that an orientation of a set of cuts points to a single structure, which is precisely the purpose of tangles: for fixed $a \in \mathbb{N}$, an orientation O of a set of cuts is *consistent* if all triples of oriented cuts have at least a objects in common:

$$\forall A, B, C \in O: |A \cap B \cap C| \geq a. \quad (1)$$

We call the parameter a the *agreement parameter*, and a consistent orientation of \mathcal{P}_Ψ is called a \mathcal{P}_Ψ -*tangle*. If clear from the context, we drop the dependency on \mathcal{P}_Ψ and simply say *tangle*.

To summarize, the tangle approach to clustering is as follows: we are given a set of initial cuts \mathcal{P} of the data set. These cuts might come naturally from the application as in the questionnaire setting, or need to be constructed in a pre-processing step. We then restrict our attention to the cuts \mathcal{P}_Ψ with bounded cost and look for tangles on \mathcal{P}_Ψ , that is, consistent orientations according to Condition (1). Each such consistent orientation corresponds to a (soft) cluster. By controlling the parameter Ψ , we can control the granularity of the clusters or even generate a hierarchical clustering.

2.2 Design choices, parameters and output

Initial cuts. The utility of tangles depends strongly on the initial set of cuts \mathcal{P} , because the tangle’s contribution is to aggregate information that is present in \mathcal{P} . If no cut in \mathcal{P} is able to separate meaningful substructures, neither will the tangles. However, choosing the set of partitions is not as critical as one might think, for two reasons: (1) **Useless cuts do not interfere with tangles:** very unbalanced cuts, such as $P = \{\{v\}, V \setminus \{v\}\}$, always get oriented towards their larger side and thus have little impact on Condition (1); meaningless cuts, such as random cuts, have high cost and thus are typically excluded for all useful choices of the parameter Ψ (see next paragraph). (2) **It is not necessary that \mathcal{P} contains high quality cuts** — otherwise the whole approach would be somewhat pointless. It is enough to have some (not necessarily many) “reasonable” initial cuts. In graph theory, \mathcal{P} is usually chosen as the set of all possible cuts. But since this is infeasible in practice, choosing the initial set of partitions \mathcal{P} requires some effort. In some cases, like the questionnaire example, there is a natural, interpretable choice for \mathcal{P} . Otherwise, the **initial cuts can be produced by a naive, fast clustering algorithm**, for which tangles then operate as a kind of boosting mechanism. We further discuss these two cases in Section 4.1.

¹Readers from graph theory will notice that our terminology and notation deviates from the standard one in the mathematical tangle literature. This is on purpose, because we considerably simplified and adapted the mathematical framework to make it as accessible as possible to the machine learning world. We provide a translation table in Supplement A.

The parameter Ψ . The parameter Ψ controls the granularity of the tangles. Restricting our attention to a subset \mathcal{P}_Ψ with a small parameter Ψ will identify large subgroups in the data. As Ψ increases, the corresponding \mathcal{P}_Ψ -tangles can identify smaller, less separated clusters, but at the same time, orientations towards larger, more separated clusters may become inconsistent. Eventually, when Ψ gets too large, we might not find any consistent orientation any more. (In the questionnaire setting, the answer to a question like "Do you wear glasses?" is independent of the mindset of a person. A cut induced by such a question will incur a high cost, hence this questions will only be included in \mathcal{P}_Ψ for a large values of Ψ . Once many such questions are included in \mathcal{P}_Ψ , it will be impossible to identify a consistent way of answering, and the tangle algorithm will tell us so.) Alternatively to fixing a single value of Ψ , we can generate a whole hierarchy of clusterings, see Section 4.2.

Consistency condition. The consistency Condition (1) is the essence of tangles, because it forces every cut to point towards the same substructure. It might seem arbitrary at first to consider the intersection of exactly three sides. However, this number has been carefully chosen: tangle theory suggests that three is the lowest number which ensures that tangles point to cohesive regions, whereas consideration of more than three merely increases computational complexity.

Agreement parameter a . The agreement parameter a controls the minimal degree to which the sides of an orientation have to agree. When chosen too small, the consistency condition induced by a may be too weak so that tangles identify substructures which we would not consider cohesive. Additionally, smaller choices of a make the computation slower. On the other hand, a should not be chosen larger than the smallest cluster that we want tangles to discover. Indeed, in practice, a should be slightly smaller than the smallest cluster that we want to identify to allow for fuzziness of the clusters. The more the cuts \mathcal{P} (resp. \mathcal{P}_Ψ) respect the cluster structure and the richer the set \mathcal{P} is, the more we can reduce a without erroneously identifying incohesive structures as tangles.

Tangles as output. Since Condition (1) only considers the intersection of triples, the intersection of all sides in an orientation can be empty. (For example in the questionnaire setting, a tangle, which corresponds to a typical way of answering, does not imply the existence of a single person who answers like this.) It is therefore inappropriate to think of tangles as subsets; rather, they point towards a region without making statements about individual objects. Consequently, the output of this algorithm is not a hard clustering, but, if desired, can be post-processed to one (Supplement D.3).

3 Theoretical results

We now propose and analyze two simple, data generating models and show that tangles can identify the ground truth in these models. Details and proofs are deferred to the supplementary material.

3.1 Questionnaire framework

In this section, we propose the following generative model for mindsets in binary questionnaires. We simulate n persons that answer m questions. We start by generating k ground-truth mindsets $\mu_1, \dots, \mu_k \in \{0, 1\}^m$. Each of the vectors μ_i describes the "typical answers" of persons of mindset i to all m questions. The entries of the mindset vectors are generated by independently throwing a fair coin. For every mindset μ_i , we generate a corresponding group V_i of n/k persons. By default, every person $v \in V_i$ answers question ℓ as indicated by $\mu_i(\ell)$, but with noise probability $p \in (0, 0.5)$ the person gives the opposite answer (independently across questions and persons). The groups then form the total population $V = \bigcup_{i=1}^k V_i$. Each question s induces a cut of V into the sets $A_s^0 = \{v \in V \mid s(v) = 0\}$ and $A_s^1 = \{v \in V \mid s(v) = 1\}$, where $s(v) \in \{0, 1\}$ denotes the answer of person v to question s ; the collection of these cuts is denoted by \mathcal{P} . We use the cost function described in Section 2.1, that is, $c(\{A, A^c\}) = \sum_{v \in A, w \in A^c} \sum_{i=1}^m \mathbb{1}\{v_i = w_i\}$. Since the cuts are induced by the questions, there is a natural one-to-one relationship between orientations of \mathcal{P} and $\{0, 1\}^m$. Using this relationship, we say that the tangles *recover* the mindsets if the set of all tangles on \mathcal{P} coincides with the set of all mindsets $\{\mu_1, \dots, \mu_k\}$. We prove in Theorem 3 that this happens with high probability for suitable parameter choices, which demonstrates the usefulness of tangles for clustering. The proof is based on the following technical assumption, which excludes that by sampling the mindsets μ_i we accidentally obtain a degenerate situation:

Assumption 1 (Mindsets are not degenerate). If $\tau \in \{0, 1\}^m$ satisfies that for all $x, y, z \leq m$ there exists a mindset μ_i such that $\tau(x) = \mu_i(x)$ as well as $\tau(y) = \mu_i(y)$ and $\tau(z) = \mu_i(z)$, then τ is a mindset, i.e. $\tau = \mu_j$ for some j .

Simulations show that under reasonable parameter choices, Assumption 1 is satisfied in the vast majority of all cases (see Supplement B.2.) We can additionally prove theoretically that for fixed k and growing m the probability of Assumption 1 being satisfied tends to 1:

Proposition 2 (Assumption 1 is true with high probability). For all $\beta \in \mathbb{R}$, if $m \geq \beta k \cdot 2^k$ is satisfied, then Assumption 1 is true with probability at least $1 - 2^{-(1-\beta)k}$.

The proof (see Supplement B.1) uses the fact that Assumption 1 holds if the following, much stronger, structural assertion holds: for each subset $M \subseteq \{\mu_1, \dots, \mu_k\}$ of mindsets there is an $i \leq m$ such that the mindsets in M are exactly the ones whose i -th coordinate is 1. Since the mindsets are chosen uniformly at random, the proposition follows by a simple application of the coupon collector bound.

We can now show that the orientations induced by the mindsets give rise to tangles, and that all tangles constructed on \mathcal{P} are mindsets (with high probability for suitable parameter choices).

Theorem 3 (1-1-Correspondence between mindsets and tangles). *Assume that the model parameters n, m, k and p and the tangle parameter a satisfy $p < 1/(k+3)$ and $a \in (pn, (1-3p)n/k)$. Let \mathcal{P} be the set of cuts induced by questions in the questionnaire. Then the following statements are true:*

1. *The probability that at least one of the mindsets does not induce a tangle is upper bounded by $km \exp(-2n(ka/n - 1 + 3p)^2/9k)$.*
2. *Given Assumption 1, the probability that there exists a spurious tangle that does not correspond to one of the original mindsets is upper bounded by $km \exp(-2n(a/n - p)^2/k)$.*

In both statements, the probability is taken over the random draw of the person's answers (not about the randomness in generating the ground truth mindsets, which only plays a role regarding Assumption 1). In particular, the probability that the set of mindsets corresponds exactly to the set of tangles tends to 1 as n tends to ∞ with fixed a/n .

The proof (see Supplement B.4) is for a slightly more general model and relies on tail bounds of the binomial distribution together with a union bound. In particular, the fact that n is large is only used to ensure that with high probability the persons' answers to the questions behave close to expectation.

Observe that Theorem 3 implies that we can exactly recover the 0-1-vectors μ_1, \dots, μ_k of the mindsets, as mentioned above. This does not necessarily imply that we can precisely reconstruct the sets V_i of persons. See Supplement D.3 for strategies to obtain such a hard clustering.

In Supplement B.3, we additionally present a noisy version of the mindset model, where we have additional noise questions that are not informative about the mindset. We present evidence that these noise questions do not hurt when looking for tangles. In Supplement B.4, we also present an extended model for bi-clustering, where not only the persons are assigned to different groups, but also the questions are grouped. For this model we can prove that we can recover the generative templates of the groups of persons (*mindsets*) as well as, independently of that, those of the groups of questions (*topics*), again for appropriate parameters.

3.2 Stochastic block model for graph clustering

The second part of our theoretical analysis concerns graph clustering in the expected graph of a stochastic block model. That is, we consider an edge-weighted complete graph G on n vertices V that consists of two equal-sized blocks V_1 and V_2 , which represent the ground-truth clusters. Edges within a block have weight p and edges between blocks have weight q , where $0 \leq q < p \leq 1$. In a standard stochastic block model, we would now sample an unweighted random graph from this model, where each edge would be chosen with the probability given in the ground truth model. In our case, we are going to perform the analysis just in expectation, as a proof of concept. We consider tangles on the set of all possible cuts \mathcal{P} with the cost function $c(\{A, A^c\}) := \sum_{u \in A, v \in A^c} w(u, v)$, where $w(u, v)$ denotes the weight of the edge between vertices u and v . Each of the two ground truth blocks V_1 and V_2 induces a natural orientation of the set of all cuts, by picking from each cut $\{A, A^c\}$ the side containing the majority of that block's vertices. We find that for reasonable choices of p, q and a there is a range of costs in which these two orientations are indeed distinct tangles. In Supplement C.5, we show how to extend the theorems in this section to uneven block sizes.

Theorem 4 (1-1-Correspondence of tangles and blocks). *Assume that the block model parameters p, q, n and the tangle agreement parameter a satisfy $p > 3qn/(n-2a)$, $a \geq 2$. Consider the set \mathcal{P} of all possible graph cuts, and the set \mathcal{P}_Ψ of those graph cuts with costs bounded by Ψ . If Ψ satisfies*

$$q \left(\frac{n}{2}\right)^2 \leq \Psi < n^2 p \left(\frac{1}{3} \left(1 + \frac{q}{p} - \frac{2a}{n}\right) \left(1 + \frac{q}{p}\right) - \frac{1}{9} \left(1 + \frac{q}{p} - \frac{2a}{n}\right)^2 \right),$$

then the two orientations of \mathcal{P}_Ψ induced by the two ground truth blocks are distinct and exactly coincide with the \mathcal{P}_Ψ -tangles.

Proof sketch. A full proof is given in Supplement C.1 and C.2. We show that $\{V_1, V_2\}$ is the only cut whose cost cannot be decreased by moving a single point across, which implies the lower bound and, by tangle theory, that there are no tangles other than the two given by the blocks. For the upper bound we analyze the structure of a lowest cost triple of cuts which would violate consistency. \square

On the other hand, if $p < 2q$ we have no chance to identify the two blocks as distinct tangles:

Theorem 5 (Non-identifiability / Necessary gap condition). *If $a \geq 2$ and $p < 2q$, then for any value Ψ and \mathcal{P}_Ψ the set of all cuts of cost at most Ψ , there exists at most one \mathcal{P}_Ψ -tangle.*

This is proven in Supplement C.3. The main argument is that if $p < 2q$ there is no cut except of $\{\emptyset, V\}$ which is a local minimum in the sense that moving any vertex from one side to the other does not decrease the cost. It is easy to see that there must be such a cut if there are at least two tangles.

4 Algorithmic framework

In this section, we present an algorithmic framework for data clustering with tangles. From a high level, this requires the following three independent steps: (1) Finding the initial set of cuts (weak partitions), (2) Identifying tangles, and (3) Post-processing tangles to a more useful output.

4.1 Constructing the initial set \mathcal{P} of cuts

Constructing the initial cuts is problem dependent, but there are two principal scenarios.

Natural cuts exist. In our running example of mindsets, every question naturally corresponds to a bipartition of the space, which we can use as our initial set of cuts. A similar setup works for any setting where objects are represented in a discrete feature space. For example, for a feature in $\{1, \dots, n\}$ we can use the partitions induced by the property whether the feature is $\geq k$, for all values of k . There are obvious extensions, for example considering conjunctions of questions or features.

Cuts by simple pre-processing. If no natural cuts exist, it is necessary to invoke another algorithm that produces the initial cuts in a pre-processing phase. In this case, tangles can be viewed as a boosting mechanism that allows us to use a fast, greedy heuristic for producing decent cuts, which then get aggregated to a strong clustering. These cuts cannot be completely random (see Supplement C.4 for a discussion of random low cost cuts in the stochastic block model) but also do not have to separate the clusters perfectly. Generally, it holds that the better the cuts, the fewer we need. On the other hand, increasing the number of cuts does not hurt the tangles (see Section 2.2 for a discussion).

4.2 Algorithm for finding tangles

Before we search for tangles, we need to set the cost function c and the agreement parameter a . A natural choice for the cost function is the sum of similarities between separated objects. Similar to fixing the *number* of clusters for hard clustering, the parameter a roughly fixes the *smallest size* of the clusters that tangles discover, see Section 2.2 for a discussion.

Once all parameters are fixed and the set of initial cuts \mathcal{P} is given, our goal is to identify all possible \mathcal{P}_Ψ -tangles for all values of Ψ . The naive approach of testing every possible orientation for consistency is infeasible. Instead, we first note that if $\Psi' < \Psi$, then the restriction of any \mathcal{P}_Ψ -tangle to $\mathcal{P}_{\Psi'}$ is also a $\mathcal{P}_{\Psi'}$ -tangle, because every triple of cuts in $\mathcal{P}_{\Psi'}$ is also a triple in \mathcal{P}_Ψ . Hence we can find the \mathcal{P}_Ψ -tangles by first finding the $\mathcal{P}_{\Psi'}$ -tangles and then extending them. The algorithm now proceeds as follows. We first sort all cuts in \mathcal{P} by increasing cost and list them as $P_1 = \{A_1, A_1^c\}, \dots, P_m = \{A_m, A_m^c\}$. The output of the algorithm is going to be a labeled binary tree as in Figure 3. Each vertex in the tree is labeled by an orientation of one particular cut. The tree is constructed in such a way that each of its vertices corresponds to exactly one tangle. Precisely, for a vertex t on level i the vertex labels along the path from the root to t form a consistent orientation of $\{P_1, \dots, P_i\}$, that is, a \mathcal{P}_Ψ -tangle for $\Psi = c(P_i)$.

We construct this *tangle search tree* by a breadth-first search. The tree is initialized by an unlabeled root on level 0. We now iterate over the P_i . In the i -th step, for both sides $A \in \{A_i, A_i^c\}$ and every node t on level $i - 1$, we check whether adding A to the tangle identified with node t is consistent. If it is, we add a child node to t , labeled with A . After we have iterated over all the cuts, we output the tree. Implementation details and pseudocode of this algorithm can be found in Supplement D.

The algorithm has complexity $O(nm^3\ell)$ where n is the number of objects in our data set, m is the number of cuts in \mathcal{P} , and ℓ is the number of leaf nodes of the tangle search tree (the tangles at the leaf nodes roughly correspond to the smallest clusters after appropriate post-processing). The parameter a only influences the complexity indirectly via ℓ , because increasing a strengthens the consistency condition and thus shrinks the size of the tree. The practical implication of the linear complexity in n is that the bottleneck for large data sets shifts towards the algorithm to find initial cuts.

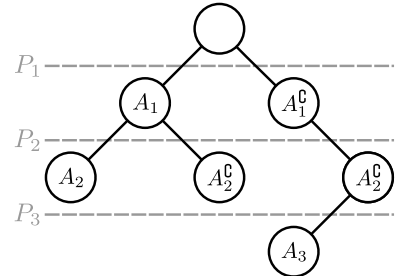


Figure 3: A tangle search tree that encodes all possible \mathcal{P}_Ψ -tangles in the node labels.

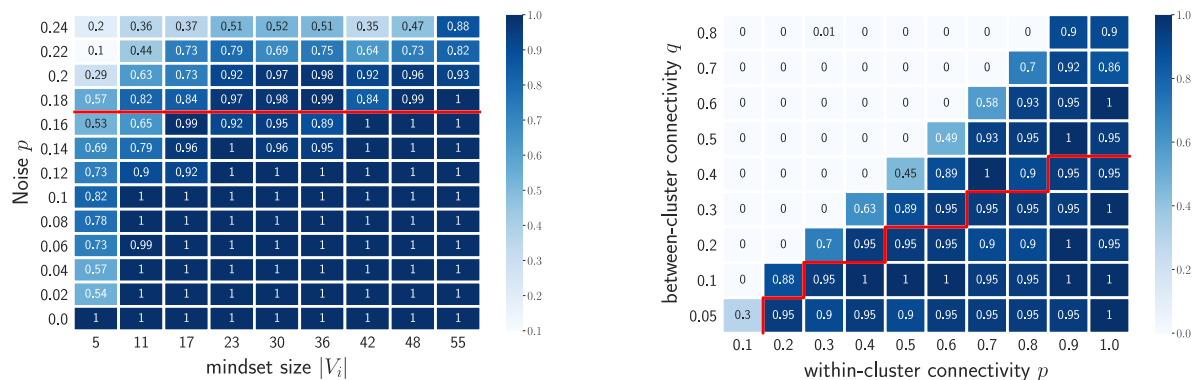
4.3 Post-processing tangles to useful output

The output of our above algorithm, the tangle search tree, reveals the hierarchical cluster structure of a data set from the point of view of the initial cuts. However, since traditional clustering is concerned with assigning individual objects to clusters, we need to post-process the tangle search tree. We propose one possible way of doing so in Supplement D.2 and D.3. For this, we first contract the paths in the tangle search tree, and then use a suitable set of cuts to softly separate the data set at each node. The result is a “**soft dendrogram**”, as depicted in Figure 2, which can easily be processed further into **heatmaps** of cluster membership or even **hard cluster assignments**.

5 Experiments

The purpose of the experiments is to demonstrate that tangles are useful for clustering in principle. In the main paper we highlight a few experimental results on the models from Section 3, many more are presented in Supplements E and F. We focus on the hard clustering task, because it is easier to evaluate, and refer to Supplement G for visualizations of our hierarchical soft clustering approach.

Experimental setup. We present the output of our algorithm for two generative models, the mindset model from Section 3.1 and the stochastic block model. We use the “adjusted Rand index” (Hubert and Arabie, 1985) to evaluate the results. For the block model we find the initial cuts using the local search heuristic presented in Fiduccia and Mattheyses (1982) (FM) with early stopping and with its required lower bound parameter chosen as 0.4 (see Supplement F.1). We use the similarity-based cost functions as in Section 3, and set the agreement parameter a to $n/6$ for the mindset and $n/4$ for the block model. For post-processing, we used the hard clustering explained in Supplement D.2.



(a) Mindset model: Rand index as a function of cluster size and noise (other parameters: $k = 2$ mindsets, $m = 40$ questions, agreement $a = |V_i|/3$). The red line shows the bound from Theorem 3 for $n \rightarrow \infty$.

(b) Block model: Rand index as a function of within- and between-cluster connectivity (other parameters: 2 blocks of 100 nodes, 50 cuts generated by FM with lower bound 0.4, agreement = 50). The red line shows the bound from Theorem 5.

Figure 4: Adjusted Rand index for tangles on two models (darker is better; 0 for random guessing, 1 for perfect recovery) with bounds from Theorems 3 and 5 as red lines. Values averaged over 10 runs.

Evaluation. Figure 4 shows the results for multiple instances of both generative models along with our theoretical bounds from Section 3. In Figure 4a, we observe that the bound for the mindsets model is almost sharp, because the performance significantly drops once the noise parameter exceeds the red line. In Figure 4b, we observe that we outperform our theoretical bound in the stochastic block model. This bound might be too pessimistic, because it is based on the set of all possible cuts; using only good cuts as produced by FM improves the performance, whereas using only bad cuts would decrease it. Simulations that confirm this behavior are shown in Supplement F.3. While a single run took only few seconds for the mindset model, it took about one minute for the block model. This supports the observation of Section 4.2 that the computational bottleneck is finding the cuts.

Assessing the size of the smallest cluster. With the agreement parameter a and post-processing of the tangle search tree, we can control the size of the smallest cluster that tangles can discover. Doing so correctly is related to the problem of deciding up to which cost a cut is still useful in separating small clusters, or simply cuts through a cluster. The agreement parameter a can achieve this by controlling how difficult it is for an orientation to satisfy the consistency condition as discussed in Section 2.2. However, another possibility is to directly restrict the maximal cost of a cut to some Ψ_{\max} . The quality of the final clustering might depend on the combination of the two parameters, corresponding

experiments can be found in Supplements E.3 and F.4. Depending on the quality of the cuts, this interplay between a and Ψ_{\max} becomes more or less relevant. If the cuts perfectly separate the clusters, the approach works well for most parameter choices. As the cuts get more rough, we can compensate with appropriate parameter choices. In Supplement H, we provide some rules of thumb on choosing the parameters that seem to work in practice.

6 Conclusion and future work

In this paper, we introduce tangles to the machine learning community. Hidden to the reader, this required a major effort of simplifying general concepts and extracting the essence that is necessary to convert the mathematical theory of tangles to a practical framework. We provide a first set of algorithms that work in practice and establish theoretical results that give provable guarantees that tangles discover the desired structure in two different statistical models (mindset model and expected stochastic block model). We consider both our algorithms and theoretic results as a first proof of concept that establish tangles as a promising tool in the field of clustering.

What we like about tangles is their flexibility: the general concept of "pointing towards a cluster" is a nice and soft formulation of a generic clustering problem, and the fact that the only input necessary is a set of weak cuts of the data makes tangles applicable in a wide range of scenarios.

There are many obvious directions for future research. On the algorithmic side, the interplay between the pre-processing phase (finding initial cuts), the tangle algorithm, and the post-processing needs to be explored much further. This also involves a more systematic understanding of how the different parameters of the algorithm interact with each other (the number and quality of initial cuts, the agreement parameter a , and the cost upper bound Ψ), and includes the complexity trade-off between pre-processing, tangle-finding phase and post-processing. On the theory side, the most intriguing question is whether it is possible to formalize the intuition that tangles provide a generic tool to convert weak to strong clusters.

Acknowledgements

This work has been supported by the German Research Foundation through the Cluster of Excellence "Machine Learning – New Perspectives for Science" (EXC 2064/1 number 390727645), the BMBF Tübingen AI Center (FKZ: 01IS18039A), and the International Max Planck Research School for Intelligent Systems (IMPRS-IS).

References

- R. Diestel. Abstract separation systems. *Order*, 35(1):157–170, 2018.
- R. Diestel. Tangles in the social sciences. *arXiv:1907.07341*, 2019.
- C. Fiduccia and R. Mattheyses. A linear-time heuristic for improving network partitions. *Conference on Design Automation*, pages 175–181, 1982.
- M. Grohe and P. Schweitzer. Computing with tangles. *Symposium on Theory of Computing (STOC)*, pages 683–692, 2015.
- L. Hubert and P. Arabie. Comparing partitions. *Journal of Classification*, 2(1), 1985.
- D. R. Karger. Global min-cuts in RNC, and other ramifications of a simple min-cut algorithm. *Symposium on Discrete Algorithms (SODA)*, pages 21–30, 1993.
- G. Karypis and V. Kumar. A fast and high quality multilevel scheme for partitioning irregular graphs. *SIAM Journal on Scientific Computing*, 20(1):359–392, 1998.
- B. Kernighan and S. Lin. An efficient heuristic procedure for partitioning graphs. *The Bell Systems Technical Journal*, 49(2), 1970.
- R. Motwani and P. Raghavan. *Randomized Algorithms*. Cambridge University Press, 1995.
- N. Robertson and P. D. Seymour. Graph minors. X. Obstructions to tree-decomposition. *Journal of Combinatorial Theory, Series B*, 52(2):153–190, 1991.

Supplementary material

A Translation between our terminology and the one used in graph theory

Tangles originate in mathematical graph theory, where they are treated in much more generality than what we need in our paper (cf. Diestel (2018) for an overview). For our work, we condensed the general theory to what we believe is the essence of tangles that is needed for applications in machine learning. Since our setting is much simpler than the general one in mathematics, we also opted for a terminology which is simpler and closer to the language of the machine learning community. In the following table we provide a glossary of the correspondences between our terminology and that of Diestel (2018).

This paper		Mathematical literature, e.g. Diestel (2018)
cuts/partitions	instance of	separations
side of a cut/oriented cut	instance of	oriented separation
cost of a cut	instance of	order of a separation
set \mathcal{P}	instance of	separation system S
O is consistent	corresponds to	O avoids $\mathcal{F} = \{\{A_1, A_2, A_3\} \mid \bigcap_{i=1}^3 A_i < a\}$
O is a \mathcal{P}_Ψ -tangle	corresponds to	O is an \mathcal{F} -tangle of \mathcal{P}_Ψ (for \mathcal{F} as directly above)
<i>not used: condition</i> $A \cap B \neq \emptyset \forall A, B \in O$	—	O is consistent
tangle search tree (<i>the output of our algorithm</i>)	—	<i>not used</i>
<i>not used</i>	—	tree of tangles (<i>a tree-like set of cuts that partitions the tangles, similar to a space-partition-tree</i>)

Furthermore, whereas we denote by \mathcal{P}_Ψ the set of all cuts from \mathcal{P} of costs *at most* Ψ , in the mathematical literature, S_k usually denotes the set of all separations from S of order *less than* k .

Note that throughout the literature there are multiple ways to denote an oriented cut. Diestel (2018), for example, comes at the topic from the angle of graph theory, closely following Robertson and Seymour (1991), and has the convention of always listing both sides (A^c, A) , where this is interpreted as *pointing from A^c towards A* . On the other hand, coming from matroid theory, Grohe and Schweitzer (2015), among others, have the custom of representing a tangle as a set of all the *small sides*, the A^c s in our terminology, which means the element-wise complements of the tangles in this paper would be tangles in their sense.

B The mindset model: proofs and extensions

B.1 Proof of Proposition 2

Every question q_i in the mindset model from Section 3.1 induces a partition of the mindsets μ_j into those satisfying $\mu_j(i) = 0$ against those with $\mu_j(i) = 1$. Note that there are 2^k distinct such partitions.

Since our mindsets are all chosen independently from each other as random 0-1-vectors, the probability that a given question induces a given partition is $1/2^k$. In particular, the probability is the same for every partition.

We are now interested in the probability that our set of m many questions induces *every* possible partition. This probability can be calculated with the common coupon-collectors-bound:

Lemma 6 (Questions induce every partition). *For every $\beta > 0$, if $m \geq \beta k \cdot 2^k$, the probability that there is one partition of the mindsets which is not induced by one of the m many questions is less than $2^{(1-\beta)k}$.*

Proof. Since the questions are all independent from each other, and induce each of the 2^k many partitions with the same probability, this model corresponds to the coupon collector's problem with 2^k many coupons. Thus, by the well known tail bound (Motwani and Raghavan, 1995), the probability that we would need more than $\beta 2^k \log(2^k)$ many questions is at most $(2^k)^{1-\beta} = 2^{(1-\beta)k}$. As $\beta 2^k \log(2^k) \leq \beta 2^k k$, this proves the claim. \square

Proof of Proposition 2. In view of Lemma 6, it remains for us to show that Assumption 1 holds once every partition of the mindsets is induced by some question.

So suppose the latter and let us show that Assumption 1 is true. Let τ be a 0-1-vector of length m with the property that for all $x_1, x_2, x_3 \leq m$ there is some mindset μ_i such that $\tau(x_j) = \mu_i(x_j)$ for $j = 1, 2, 3$. For a contradiction, suppose that τ is not itself a mindset.

Consider a triple $x_1, x_2, x_3 \leq m$ such that there are as few mindsets μ_i as possible satisfying $\tau(x_j) = \mu_i(x_j)$ for $j = 1, 2, 3$. By assumption there is at least one such mindset, say μ_1 . Since every partition of the mindsets is induced by some question, there is an $x_4 \leq m$ such that $\mu_i(x_4) = \mu_i(x_1)$ for all $i \neq 1$ and $\mu_1(x_4) \neq \mu_1(x_1)$. If $\tau(x_4) \neq \mu_1(x_4)$ the triple x_2, x_3, x_4 would contradict the choice of x_1, x_2, x_3 . Therefore $\tau(x_4) = \mu_1(x_4)$. But then the triple x_1, x_4, x_5 , for some x_5 such that $\tau(x_5) \neq \mu_1(x_5)$, again contradicts the choice of x_1, x_2, x_3 . \square

B.2 Assumption 1 in simulations

To verify Assumption 1 in practice, we ran the following experiment: For a range of parameters k and m we independently sampled 1000 instances of the basic mindset model without topics. We then determined the share of cases where our Assumption 1 was violated. For parameters where no such violation appeared among this sample of 1000, we sampled another 4000 instances and determined the share of violations of the assumption among those total 5000 experiments. This additional sampling was done to obtain a higher resolution for the boundary behavior.

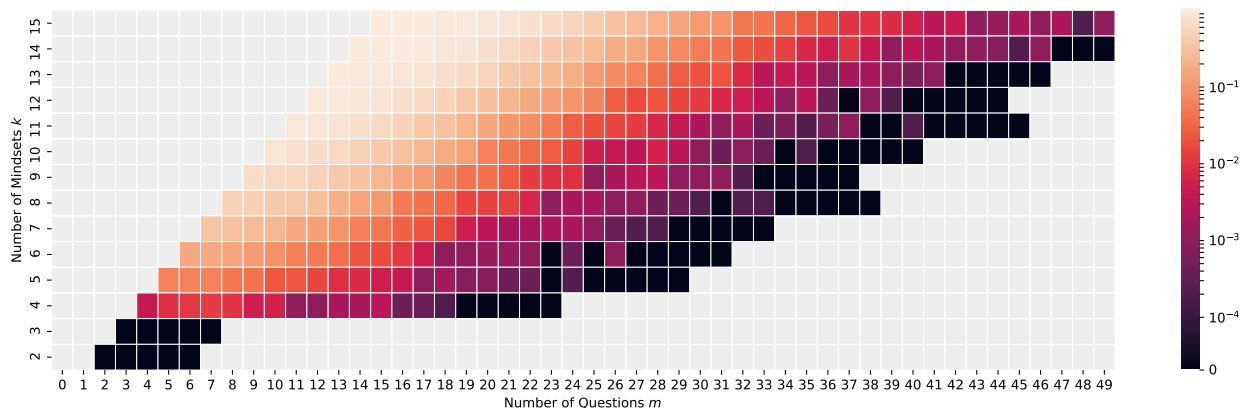


Figure 5: Relative amount of cases where Assumption 1 was violated.

The parameter k was chosen as $k = 2, 3, \dots, 15$. For the parameter m we began with $m = k$ and then increased m in steps of 1 until no violation of Assumption 1 was found for five values of m in a row. Since the share of violations of Assumption 1 is asymptotically decreasing in m , it may be assumed that no significant number of violations occurs for larger values of m .

The results of these simulations are shown in Figure 5. From these results we can tell that Assumption 1 constitutes no restriction for 2 and 3 mindsets and that for 10 mindsets, for example, taking at least 36 questions is enough to have Assumption 1 with very high probability. We conclude that while this assumption is necessary to prove Corollary 10 it poses no serious restriction under practical circumstances.

B.3 Noise questions have higher expected cost and thus do not hurt

In the simple mindset model, all questions are equally “informative” about the mindsets, and for this reason the tangles could be built on the cuts induced by all the questions. However, this is quite unrealistic in practice: there will always be questions in a questionnaire that are not relevant to identify a particular mindset. For this reason, we now extend the model by introducing additional questions that do not provide any information regarding the mindsets. Obviously, the tangles do not know in advance which of the questions are informative and which ones are not, so it will be interesting to see whether they can figure it out and still recover the correct mindsets. The mechanism to use here is to restrict the set of all cuts to “low-cost” cuts.

Formally, the model is as follows: Additionally to the m questions which the populace answers mostly according to their respective mindsets, we may add a small number m' of questions to our set \mathcal{P} which every person answers at random – that is answers yes with probability $1/2$. In a real-world example we would think of these questions as something akin to “Are you male or female” which may not have any correlation with the other questions.

If our tangles would need to orient these questions, this would of course potentially violate consistency, however, what we are going to show is that, if we consider a sensible cost-function on the set of questions then the expected costs of these noise questions will be substantial higher than the costs of other questions. Thus even if our mindsets might fail to correspond to a tangle of all questions, there will still be a large range of values of Ψ for which the mindsets correspond to distinct \mathcal{P}_Ψ -tangles.

Let us verify that the expected cost of a noise question is higher than the expected cost of a non-noise question. In our model, a noise question is simply a random cut of the populace. On the other hand a real question is expected to split each mindset into chunks of size p and $1 - p$, respectively.

Let $\text{sim}: V \times V \rightarrow \mathbb{R}$ be a similarity function, for instance the number of questions answered in the same way by the given pair of persons. The cost $c(q)$ of a question q is then given by the sum of all $\text{sim}(v_1, v_2)$, going over all pairs $v_1, v_2 \in V$ of persons which disagree on q .

For two persons $x, y \in V$ chosen uniformly at random, we let d_i and d_e be the expected similarity of x and y in the cases where x and y belong to the same or to different mindsets, respectively:

$$d_i := \mathbb{E}[\text{sim}(x, y) \mid x, y \in V_j \text{ for some } j]$$

and

$$d_e := \mathbb{E}[\text{sim}(x, y) \mid x, y \text{ in distinct } V_j].$$

Recall that k is the number of mindsets and let $n_1 = \dots = n_k$ be the number of persons in each mindset. The expected cost of a noise and a "real" question then works out to

$$\begin{aligned} \mathbb{E}[|c(q_{\text{noise}})|] &= \frac{1}{2} \cdot k \binom{n_1}{2} \cdot d_i + \binom{k}{2} n_1^2 \cdot \frac{1}{2} \cdot d_e, \\ \mathbb{E}[|c(q_{\text{real}})|] &= 2p(1-p) \cdot k \binom{n_1}{2} \cdot d_i + \binom{k}{2} n_1^2 \cdot \frac{1}{2} \cdot d_e. \end{aligned}$$

The common term $\binom{k}{2} n_1^2 \cdot d_e/2$ comes from the fact that, for noise questions and meaningful questions alike, a pair of persons picked randomly from distinct mindsets are as likely to answer that question the same as they are to answer it differently.

The difference in these terms is in the leading factor, $1/2$ or $2p(1-p)$, of $k \binom{n_1}{2} \cdot d_i$ which is the probability for a random pair of persons from the same mindset to answer the question differently. Observe that – as expected – the expressions for noise and for non-noise questions agree for $p = 1/2$. For $p \neq 1/2$ they differ as follows: the term $2p(1-p)$ becomes smaller than $1/2$. Thus the expected cost of a non-noise question is always lower than that of a noise question, unless $p = 1/2$ (which would make every question a noise question.)

B.4 The mindsets-topics biclustering model and proof of Theorem 3 in the main paper

In this section, we are going to prove the main theorems from Section 3.1. In fact we are not using the model from Section 3.1 but instead a slightly more general model, which will allow us to actually show a biclustering result, by also assuming that every question belongs to a specific topic and then trying to not only recover the mindsets but also the topics.

This model works as follows. We fix a number k of mindsets and l of topics. Then we generate the ‘base answer’ of each mindset to each topic by flipping a coin. In other words, we have computed a random binary $k \times l$ -matrix.

We then generate a population V of n persons consisting of $n_1 = \dots = n_k$ many persons V_i for each mindset μ_i . Likewise we generate a questionnaire Q of m questions consisting of $m_1 = \dots = m_l$ questions Q_j belonging to each topic θ_j .

It remains to decide how each person should answer each question. For this we pick noise probabilities p and q . To start with, each person $v \in V_i$ answers each question $x \in Q_j$ according to the ‘base answer’ of mindset μ_i to topic θ_j . Then, for every person $v \in V$, we flip the answers of v to all questions belonging to a topic θ_j with probability p for each topic. Likewise, for every question $x \in Q$, we flip the answers to x given by all the persons belonging to a mindset μ_i with probability q for each mindset. The order of these two flips is obviously immaterial. The result of this is a binary $n \times m$ -matrix containing the answers of each person to each question.

Finally, for good measure, we fix a small noise probability r and flip each entry of the $n \times m$ -matrix independently with probability r . In other words, for each person and each question we flip that person’s answer with probability r .

Each question defines a partition of V into those who answer 0 and those who answer 1 to that question. Dually, each person defines a partition of Q into those questions answered with 0 and those answered with 1 by that person. In particular this model is symmetric in the sense that we could replace the role of the mindsets and questions by the role of the topics and persons and vice versa. We can now consider the questions as cuts of V , the set of persons, and

calculate the tangles with agreement parameter a_Q for these cuts – which should correspond to the mindsets – and, simultaneously, consider the persons as cuts of Q and calculate the tangles with agreement parameter a_V for these cuts – which should correspond to the topics.

Observe that the model described in Section 3.1 corresponds to this model if we choose $p = 0$, $q = 1/2$ and $l = 1$ and only consider tangles of the set of cuts of V induced by the questions, with agreement parameter $a = a_Q$. In that case r in this model corresponds to the p from Section 3.1.

Given a mindset μ_i , the orientation of the questions induced by that mindset is the orientation which orients each question $x \in Q$ towards the answer that a person in V_i would give if non of that person's answers got flipped, i.e. for $p, r = 0$. Similarly the orientation induced by a topic θ_j on V orients each person towards the answer which a question in Q_i would receive from that person for $q, r = 0$.

Let us start by verifying that the mindsets and topics define tangles with high probability.

B.4.1 Mindsets/Topics give tangles

Lemma 7 (Mindsets/Topics are tangles in the biclustering setup). *Let k and l be fixed and let $\alpha_Q = a_Q/n$ and $\alpha_V = a_V/m$ be the agreement parameters as fractions of n or m respectively. If $1 - 3(p + r) + 6pr > k\alpha_Q$ then the probability that there is a mindset which does not define a tangle is at most*

$$mk \exp\left(-\frac{2n}{9k}(k\alpha_Q - 1 + 3p + 3r - 6pr)^2\right),$$

which tends to 0 as n goes to ∞ , as long as m is not larger than n . Similarly, if $1 - 3(q + r) + 6qr > l\alpha_V$, then the probability that there is a topic which does not define a tangle is at most

$$nl \exp\left(-\frac{2m}{9l}(l\alpha_V - 1 + 3q + 3r - 6qr)^2\right),$$

which tends to 0 as m goes to ∞ , as long as n is not larger than m .

Thus, if both inequalities hold, then for $m = n$ large enough both the mindsets and the topics define tangles almost surely.

Proof. We shall verify this for the mindsets; exchanging the appropriate letters will give a proof for the topics. If some mindset μ_i is not a tangle then it contains a triple of questions whose intersection has size at most a_Q . Hence by the pigeon-hole principle for at least one of these three questions at most $(2n_i + a_Q)/3$ of the n_i persons in V_i answered that question as μ_i does.

Each person in V_i answers a question as μ_i does with probability $(1 - p)(1 - r) + pr$. Observe that our assumption that $1 - 3(p + r) + 6pr > k\alpha_Q$ is equivalent to $(2n_i + a_Q)/3 < (1 - p)(1 - r)n_i + prn_i$. We can therefore apply Hoeffding's tail bound on the binomial distribution with success percentage $(1 - p)(1 - r) + pr$ to find that

$$\begin{aligned} \mathbf{P}\left[X \leq \frac{2n_i + a_Q}{3}\right] &\leq \exp\left(-2\frac{\left(\frac{2n_i + a_Q}{3} - ((1 - p)(1 - r) + pr)n_i\right)^2}{n_i}\right) \\ &= \exp\left(-\frac{2n}{9k}(k\alpha_Q - 1 + 3p + 3r - 6pr)^2\right), \end{aligned}$$

where X is the random variable counting the number of persons in V_i that answer a fixed question as μ_i does. Note that we used $a_Q = n\alpha_Q = kn_i\alpha_Q$ here.

Since there are k mindsets and m questions, by the union bound we obtain that the probability of the event that there is some question for which few persons answer following their mindset is at most

$$mk \exp\left(-\frac{2n}{9k}(k\alpha_Q - 1 + 3p + 3r - 6pr)^2\right).$$

Consequently so is the probability that some mindset is not a tangle. □

In particular this implies the following corollary, which proves the first part of Theorem 3

Corollary 8 (Mindsets give tangles). *In the original model from Section 3.1, if $a = \alpha n$ and $p < (n - ka)/(3n)$, then the probability that there is one of the k mindsets which does not induce a tangle is bounded above by $km \exp(-2n)/(9k)(k\alpha - 1 + 3p)^2$.*

Proof. If we set $p = 0$, $q = 1/2$, $l = 1$, $a_Q = a$ and replace r by the p from Corollary 8, then the statement of the first half of Lemma 7 corresponds exactly to the statement of Corollary 8. □

B.4.2 Only tangles from mindsets/topics

The next ingredient we need is the assertion that the only triples with large intersection are those contained in some mindset (or the dual equivalent).

Lemma 9 (Every triple with large intersection is contained in a mindset/topic). *If k, l , and tangle agreement fractions $\alpha_Q := a_Q/n$ and $\alpha_V := a_V/m$ are fixed, then for $p + r - 2pr \leq \alpha_Q$ we have that the probability that there exist sides of cuts $A_1 := A_{x_1}^{y_1}$, $A_2 := A_{x_2}^{y_2}$ and $A_3 := A_{x_3}^{y_3}$ with intersection $|A_1 \cap A_2 \cap A_3| \geq a_Q$ but no mindset μ which incorporates these, i.e. with $\mu(x_i) = y_i \forall i \in \{1, 2, 3\}$, is at most*

$$mk \exp \left(-\frac{2n}{k} (p + r - 2pr - \alpha_Q)^2 \right),$$

which tends to 0 for $m \leq n$ and n going to infinity.

Similarly, if $q + r - 2qr \leq \alpha_V$ the probability that there exist $B_{x_1}^{y_1}$, $B_{x_2}^{y_2}$ and $B_{x_3}^{y_3}$ with intersection of size at least a_V but we have no topic θ with $\theta(x_i) = y_i \forall i \in \{1, 2, 3\}$ is at most

$$nl \exp \left(-\frac{2m}{l} (q + r - 2qr - \alpha_V)^2 \right),$$

which tends to 0 for $n \leq m$ with m going to infinity.

Proof. We shall verify this for the mindsets; exchanging the appropriate letters will give a proof for the topics. So suppose that there are such A_1, A_2, A_3 with $|A_1 \cap A_2 \cap A_3| > a_Q$. Then there is, by the pigeon-hole principle, a mindset μ_i for which at least a_Q/k many persons from V_i lie in $A_1 \cap A_2 \cap A_3$. If this mindset does not incorporate this triple, then it does not incorporate one of the questions, say $\mu_i(x_1) \neq y_1$.

We are going to compute the probability that there is some such A_x^y and a mindset μ_i where more than $n_i - a_Q/k$ many persons from V_i lie in A_x^y , but $\mu_i(x) \neq y$. This calculation is similar to the one in Lemma 7.

Each person in V_i answers a question as μ_i does with probability $(1-p)(1-r) + pr$. Since it follows from $p + r - 2pr \leq \alpha_Q$ that $n_i - a_Q/k \leq (1-p)(1-r)n_i + prn_i$, we can apply Hoeffding's tail bound on the binomial distribution with success probability $(1-p)(1-r) + pr$ to find that

$$\begin{aligned} \mathbf{P}[X \leq n_i - \frac{a_Q}{k}] &\leq \exp \left(-2 \frac{(n_i - \frac{a_Q}{k} - ((1-p)(1-r) + pr)n_i)^2}{n_i} \right) \\ &= \exp \left(-\frac{2n}{k} (p + r - 2pr - \alpha_Q)^2 \right), \end{aligned}$$

where X is the random variable counting the number of persons in V_i that answer a fixed question as μ_i does. Note that we used $a_Q = n\alpha_Q = kn_i\alpha_Q$ here.

Since there are k mindsets and m questions, by the union bound we obtain that the probability of the event that there is some such A_x^y and μ_i is at most

$$mk \exp \left(-\frac{2n}{k} (p + r - 2pr - \alpha_Q)^2 \right),$$

The probability that there exists a triple A_1, A_2, A_3 as in the claim is also at most this value since – as argued above – the A_1 in such a triple is such an A_x^y , witnessed by μ_i . \square

By choosing the right parameters we can use Lemma 9 to prove a corollary which verifies the second half of Theorem 3:

Corollary 10 (Only tangles from mindsets). *In the original model from Section 3.1, if $a = \alpha n$ and $p < a/n$, then, given Assumption 1, the probability that there is a tangle which is not a mindset is bounded above by $km \exp(-2(\alpha - p)^2 n/k)$.*

Proof. By Assumption 1, for a tangle τ which does not correspond to a mindset there need to exist x_1, x_2, x_3 such that for $y_i = \tau(x_i)$ we have that for $A_1 := A_{x_1}^{y_1}$, $A_2 := A_{x_2}^{y_2}$ and $A_3 := A_{x_3}^{y_3}$ that $|A_1 \cap A_2 \cap A_3| \geq a_Q$ but no mindset μ incorporate A_1, A_2, A_3 , i.e. there is no μ with $\mu(x_i) = y_i \forall i \in \{1, 2, 3\}$.

If we set $p = 0$, $q = 1/2$, $l = 1$, $a_Q = a$ and replace r by the p from Corollary 10, then by the first half of Lemma 9, the probability that there are such x_1, x_2, x_3 is at most $km \exp(-2(\alpha - p)^2 n/k)$ which verifies the statement of Corollary 10. \square

Proof of Theorem 3. Observe that the inequality $p < 1/(k + 3)$, which holds by assumption, is equivalent to $p < (1 - 3p)/k$. Consider any α with $p < \alpha < (1 - 3p)/k$, and note that $\alpha \in (0, 1)$. Then for every choice of n and m we have with $a = \alpha n$ that

$$\frac{n - ka}{3n} = \frac{1 - k\alpha}{3} > \frac{1 - k\frac{1-3p}{k}}{3} = p,$$

which is the assumption of Corollary 8. Moreover $p < \alpha$, which was (together with Assumption 1) the assumption of Corollary 10. \square

B.4.3 Technical assumptions in the biclustering model

Let us now show that under technical assumptions similar to Assumption 1 we can even show that in this biclustering model the tangles correspond exactly to the mindsets or topics respectively. These technical assumptions are as follows:

(A) *Every orientation of the questions whose triples are each contained in some mindset is itself a mindset.*

And likewise for topics:

(B) *Every orientation of the persons whose triples are each contained in some topic is itself a topic.*

Under these assumptions we can show:

Proposition 11 (Tangles equal mindsets/topics in the biclustering setup). *For fixed k and l and noise probabilities p, q, r such that*

$$p + r - 2pr < \frac{1 - 3(p + r) + 6pr}{k}$$

there is, for each $\varepsilon > 0$ a value of m and a choice of α_Q such that, in the biclustering model and under Assumption (A) the tangles of the set of cuts Q with agreement α_Q are precisely the mindsets with probability at least $1 - \varepsilon$. Similarly, if

$$q + r - 2qr < \frac{1 - 3(q + r) + 6qr}{l}$$

there is a value of m and a choice of α_V such that the tangles of the set of cuts V with agreement α_V are precisely the topics with probability at least $1 - \varepsilon$. In particular, if both these inequalities hold, there are such choices for $n = m$ which results in the tangles being, with high probability, precisely the mindsets and topics, respectively.

Proof. Pick α_Q and α_V in between the left-hand and the right-hand side of the inequalities in the assumption. Then by Lemma 7 and Lemma 9 we have for sufficiently large n , respectively m that with high probability each mindset, respectively each topic, defines a tangle, and moreover that every triple of questions, or persons respectively, with large intersection lies in some mindset, respectively topic. The latter together with the Assumptions (A) or (B), respectively, ensures that there are no tangles apart from the mindsets, respectively the topics, as desired. \square

Let us end this section with a set of parameters for which the Assumptions (A), (B) hold almost surely.

Lemma 12 (The technical assumptions hold with high probability in the biclustering setup). *For parameters $k, l, p, q,$ and r as in Proposition 11, if q is positive, then for m going to infinity (and therefore n going to infinity as well), we almost surely have Assumption (A). Similarly, if p is positive, then with n (and therefore m) going to infinity we almost surely have Assumption (B).*

Proof. Let us show that we have Assumption (A) almost surely. For this pick n and m large enough that the assertion of Lemma 9 holds and that with high probability each partition of the k mindsets is induced by some question. (Note that we use $q > 0$ for the latter, since l is fixed but m is not.)

Let us deduce Assumption (A). For this, let τ be some orientation each of whose triples lies in some mindset. For a contradiction, suppose that τ is not itself a mindset.

Consider a triple (A_1, A_2, A_3) contained in τ that lies in as few mindsets as possible. By assumption this triple is contained in at least one mindset, say, ρ . By assumption there is a question A'_1 which every mindset except ρ answers in the same way as A_1 .² If τ contains A'_1 we would obtain a triple (A'_1, A_2, A_3) contained in fewer mindsets than our original choice. Therefore $A'_1 \notin \tau$. But then A_1 and A'_1 , together with any question on which τ and ρ differ, yields a triple in τ not contained in any mindset. \square

²We mean: every mindset other than ρ contains A'_1 if and only if it contains A_1 .

C The stochastic block model: proofs of the main results

We will consider tangles in the universe of cuts of the complete weighted graph as described in section 3.2: We take the set \mathcal{P} of all partitions $P = \{A, A^c\}$ of V . The cost of such a partition is the sum over the weights of edges between A and A^c . If we denote $\alpha_i = |A \cap V_i|/|V_i|$, this gives us, as $|V_1| = |V_2| = n/2$:

$$c(\{A, A^c\}) = \frac{n^2}{4} (p(\alpha_1 - \alpha_1^2 + \alpha_2 - \alpha_2^2) + q(\alpha_1 + \alpha_2 - 2\alpha_1\alpha_2)). \quad (\text{O})$$

C.1 Blocks induce distinct tangles

In this subsection we will compute the maximum value of Ψ for which the two orientations of \mathcal{P}_Ψ (the set of all cuts of cost at most Ψ) induced by V_1 and V_2 respectively are indeed tangles, i.e. do not contain any triples with small intersection of their right sides, and we will furthermore compute the minimum value of Ψ for which the two tangles defined by the blocks are distinct. The result will be a range for the value of Ψ in which clustering with tangles returns tangles corresponding to V_1 and V_2 .

The latter part, finding the Ψ -values that result in distinct tangles, will amount to computing the cost of the cut $\{V_1, V_2\}$ thanks to tangle theory.

To find the maximum value of Ψ for which the orientations induced by V_1 and V_2 are \mathcal{P}_Ψ -tangles we shall compute the minimum cost of a *forbidden triple* in these orientations i.e. a triple which violates a -consistency. This we will do as follows: suppose that A, B, C is a forbidden triple in the orientation given by V_1 . This means that each of A, B , and C contains more than half of V_1 , but their intersection contains at most a many vertices from V_1 . We will manipulate this triple to take a specific form without increasing the cost of the cuts involved, and then compute the minimum possible cost of a triple taking this specific form.

The shape we are aiming for is this: two of those sets contain V_2 and about two-thirds of V_1 , the third one contains two thirds of V_1 and nothing else. Crucially none of the three sets cuts through V_2 .

Suppose that, say, A contains the lowest percentage of V_2 out of A, B , and C . Then we move all of V_2 to A^c , i.e. we replace A with $A \setminus V_2$. For the other two sets we replace them with $B \cup V_2$ and $C \cup V_2$. For certain values of p and q this operation only decreases the cost of the cuts induced by these three sets. The resulting new triple is still contained in the orientation given by V_1 , and will still be a ‘forbidden triple’. All we have to do, then, is compute the lowest possible value of Ψ at which triples of this shape can appear. For that we will show by optimization that the lowest cost for the cuts induced by these sets is achieved if each of them contains roughly two-thirds of V_1 .

The following lemma says that (for a certain range of parameters) the cost of cutting through both blocks is made smaller by only cutting through one block and moving the other block entirely to one side of the cut.

Lemma 13 (Not cutting through a block reduces the cost). *Let $P = \{A, A^c\}$ be a cut, and let $\alpha_i = |A \cap V_i|/|V_i|$ and $\beta_i = |A^c \cap V_i|/|V_i| = 1 - \alpha_i$. If $\alpha_2 \geq (1 - 2\alpha_1)q/p$, then $c(\{A \cup V_2, A^c \setminus V_2\}) \leq c(P)$. Similarly, if $\beta_2 \geq (1 - 2\beta_1)q/p$, then $c(\{A \setminus V_2, A^c \cup V_2\}) \leq c(P)$.*

Proof. For $\alpha_2 = (1 - 2\alpha_1)q/p$ we have by (O), that

$$\begin{aligned} & c(P) \\ &= \frac{n^2}{4} (p(\alpha_1 - \alpha_1^2 + \alpha_2 - \alpha_2^2) + q(\alpha_1 + \alpha_2 - 2\alpha_1\alpha_2)) \\ &= \frac{n^2}{4} \left(p(\alpha_1 - \alpha_1^2 + \frac{(1 - 2\alpha_1)q}{p} - (\frac{(1 - 2\alpha_1)q}{p})^2) + q(\alpha_1 + \frac{(1 - 2\alpha_1)q}{p} - 2\alpha_1 \frac{(1 - 2\alpha_1)q}{p}) \right) \\ &= \frac{n^2}{4} \left(p(\alpha_1 - \alpha_1^2) + (1 - 2\alpha_1)q - \frac{(1 - 2\alpha_1)^2 q^2}{p} + q(\alpha_1 + \frac{(1 - 2\alpha_1)q}{p} - 2\alpha_1 \frac{(1 - 2\alpha_1)q}{p}) \right) \\ &= \frac{n^2}{4} \left(p(\alpha_1 - \alpha_1^2) + q((1 - 2\alpha_1) - \frac{(1 - 2\alpha_1)^2 q}{p} + \alpha_1 + \frac{(1 - 2\alpha_1)q}{p} - 2\alpha_1 \frac{(1 - 2\alpha_1)q}{p}) \right) \\ &= \frac{n^2}{4} \left(p(\alpha_1 - \alpha_1^2) + q(1 - \alpha_1) + \frac{q}{p} ((-1 + 4\alpha_1 - 4\alpha_1^2 + 1 - 2\alpha_1 - 2\alpha_1 + 4\alpha_1^2)) \right) \\ &= \frac{n^2}{4} (p(\alpha_1 - \alpha_1^2) + q(1 - \alpha_1)) = c(\{A \cup V_2, A^c \setminus V_2\}) \end{aligned}$$

Now if we consider (O), for fixed n, p, q, α_1 as a real-valued function f mapping α_2 to $c(\{A, A^c\})$, then this is a quadratic function with a unique maximum. Thus by $f(1) = f((1 - 2\alpha_1)q/p)$ we have $f(x) \geq f(1)$ for every $(1 - 2\alpha_1)q/p \leq x \leq 1$, i.e. for $\alpha_2 \geq (1 - 2\alpha_1)q/p$ we have that $c(\{A \cup V_2, A^c \setminus V_2\}) \leq c(P)$.

The argument for $\beta_2 \geq (1 - 2\beta_1)q/p$ is analogous. □

This lemma computes the lowest possible cost of a forbidden triple of the shape described above.

Lemma 14 (Bound on the costs of a forbidden triple not cutting through a block). *For $q/p \leq 1/2$, if A, B, C are such that they each contain more than half of V_1 , their intersection has size $\leq a$, and V_2 is a subset of A^c, B , and C , then the minimum possible value of $\max\{c(\{A, A^c\}), c(\{B, B^c\}), c(\{C, C^c\})\}$ is*

$$\frac{n^2}{4}p \left(\frac{1}{3}(1+r-x)(1+r) - \left(\frac{1+r-x}{3}\right)^2 \right), \text{ where } r = \frac{q}{p}, x = \frac{2a}{n},$$

with some such triple attaining this bound (up to discretization).

Proof. This minimal possible value is attained by the following:

Fractionally, we can cover V_1 by four sets A_1, A_2, A_3 and X where

$$\begin{aligned} |X| &= a \\ |A_2| &= |A_3| = \alpha \cdot |V_1| & \alpha &= \frac{1}{3}(1+r-x). \\ |A_1| &= (\alpha - r)|V_1| \end{aligned}$$

Consider now the three sets $A = V_1 \setminus A_1, B = A_2^c$ and $C = A_3^c$. We are going to calculate their costs.

By (O) we have for B and C

$$\begin{aligned} c(\{B, B^c\}) &= c(\{C, C^c\}) \\ &= \frac{n^2}{4} (p(\alpha - \alpha^2) + q(\alpha)) \\ &= \frac{n^2}{4} \left(p\left(\frac{1}{3}(1+r-x) - \left(\frac{1}{3}(1+r-x)\right)^2\right) + q\frac{1}{3}(1+r-x) \right) \\ &= \frac{n^2}{4} p \left(\frac{1}{3}(1+r-x) - \left(\frac{1}{3}(1+r-x)\right)^2 + r\frac{1}{3}(1+r-x) \right) \\ &= \frac{n^2}{4} p \left(\frac{1}{3}(1+r-x)(1+r) - \left(\frac{1}{3}(1+r-x)\right)^2 \right) \\ &= \frac{n^2}{4} p (\alpha(1+r) - \alpha^2). \end{aligned}$$

For A we also get

$$\begin{aligned} c(\{A, A^c\}) &= \frac{n^2}{4} (p((\alpha - r) - (\alpha - r)^2) + q((\alpha - r) + 1 - 2(\alpha - r))) \\ &= \frac{n^2}{4} p (\alpha - r - (\alpha - r)^2 + r((\alpha - r) + 1 - 2(\alpha - r))) \\ &= \frac{n^2}{4} p (\alpha - r - \alpha^2 + 2r\alpha - r^2 + r\alpha - r^2 + r - 2r\alpha + 2r^2) \\ &= \frac{n^2}{4} p (\alpha + r\alpha - \alpha^2) \\ &= \frac{n^2}{4} p (\alpha(1+r) - \alpha^2). \end{aligned}$$

Let us now argue that this is indeed the minimal possible value. For this we first calculate the cost $\{A, A^c\}$ would have if $|A^c \cap V_1| = |V_1|/2$:

$$\begin{aligned} c(\{A, A^c\}) &= \frac{n^2}{4} \left(p\left(1 - 1^2 + \frac{1}{2} - \frac{1}{2}\right) + q\left(1 + \frac{1}{2} - 2 \cdot 1 \cdot \frac{1}{2}\right) \right) \\ &= \frac{n^2}{4} \left(p\frac{1}{4} + q\frac{1}{2} \right) \\ &= \frac{n^2}{4} p \left(\frac{1}{4} + \frac{r}{2} \right) \end{aligned}$$

Observe for later that

$$\left(\frac{1}{3}(1+r-x)(1+r) - \left(\frac{1}{3}(1+r-x)\right)^2\right) \leq \left(\frac{2}{9}(1+r)^2\right) \leq \frac{1}{4} + \frac{r}{2} \quad (\text{C})$$

for $0 < r \leq 1/2$.

Moreover, by the calculations in the proof of Lemma 13, for fixed p, q, n and $\alpha_1 = 0$ the quadratic function given by (O) has its maximum at

$$\frac{1 + \frac{(1-2\alpha_1)q}{p}}{2} > \frac{1}{2}.$$

Thus this function is monotone in the interval between 0 and $1/2$. Therefore, if A, B, C would be chosen such that $\max\{c(\{A, A^c\}), c(\{B, B^c\}), c(\{C, C^c\})\}$ is smaller than $n^2 p (\alpha(1+r) - \alpha^2)/4$, both $|B^c \cap V_1|/|V_1|$ and $|C^c \cap V_1|/|V_1|$ need to be smaller than α . Therefore, in order for A, B, C to be a forbidden triple, $|A^c \cap V_1|/|V_1|$ needs to be larger than $(\alpha - r)|V_1|$. Since the function given by (O) is quadratic, and, by (C), its value at $1/2$ is larger than its value at $(\alpha - r)$, this would imply that the cost of $\{A, A^c\}$ is larger than $n^2 p (\alpha(1+r) - \alpha^2)/4$, contradicting the assumption. \square

This lemma puts the bounds of the previous two lemmas together to ensure that the blocks define tangles.

Lemma 15 (Blocks are tangles). *If $p > 3qn/(n - 2a)$ and*

$$\Psi \leq \frac{n^2}{4} p \left(\frac{1}{3}(1+r-x)(1+r) - \left(\frac{1+r-x}{3}\right)^2 \right),$$

then $\tau_{\Psi}^1, \tau_{\Psi}^2$ are \mathcal{P}_{Ψ} -tangles.

Proof. Suppose for a contradiction that $A, B, C \in \tau_{\Psi}^1$ such that $|A \cap B \cap C| < a$ and such that the maximal cost of one of the three is as small as possible. In particular, since $|A \cap B \cap C| \leq a$, all but at most a vertices of V_2 need to lie in one of the sets A^c, B^c, C^c . Therefore by pigeon hole principle one of those three sets must contain at least $(|V_2| - a)/3$ of them.

However, by Lemma 13, we may now suppose without loss of generality, that this set contains all of V_2 , so let us suppose that $A^c \supseteq V_2$. But now we may additionally suppose that $B^c \cap V_2 = \emptyset, C^c \cap V_2 = \emptyset$ by Lemma 13, since those α satisfy $\alpha_1 > 1/2$ and therefore $\alpha_2 \geq 0 \geq (1 - 2\alpha_1)q/p$. Thus A, B, C is of the same form as in Lemma 14, and thus its maximal cost is minimized by

$$\frac{n^2}{4} p \left(\frac{1}{3}(1+r-x)(1+r) - \left(\frac{1+r-x}{3}\right)^2 \right).$$

The argument for τ_{Ψ}^2 is analogous. \square

This lemma gives a sharp bound on the Ψ -values for which the tangles defined by the blocks are different.

Lemma 16 (Orientations induced by the blocks are distinct). *If $p \geq 2q$, then $\tau_{\Psi}^1 = \tau_{\Psi}^2$ if and only if $\Psi \leq qn^2/4 = c(\{V_1, V_2\})$.*

Proof. The tangles defined by V_1 and V_2 orient $\{V_1, V_2\}$ differently. Since the cost of this cut is $qn^2/4$ the two tangles are distinct as soon as they orient this cut, i.e. if $\Psi > qn^2/4$.

For the converse it suffices to show that $\{V_1, V_2\}$ is of minimum cost among all cuts that are oriented differently by the two tangles. To see this consider a cut $\{A, A^c\}$ that is oriented differently by the two tangles. Then A , say, contains more than half of V_1 and A^c more than half of V_2 . Therefore we are able to apply Lemma 13. By doing so twice we can move all of V_1 into A and then all of V_2 into A^c without increasing the cost, giving $c(\{V_1, V_2\}) \leq c(\{A, A^c\})$. \square

C.2 Every tangle is induced by a block

Theorem 17 (Every tangle is induced by a block). *If $p \geq 2q$, then for any Ψ and any agreement parameter $a \geq 2$, every \mathcal{P}_{Ψ} -tangle for \mathcal{P}_{Ψ} the set of all cuts of cost at most Ψ is an orientation induced by one of the blocks. In particular, there are at most two distinct \mathcal{P}_{Ψ} -tangles.*

Proof. Suppose for a contradiction that for some $a \geq 2$ an orientation τ of \mathcal{P}_Ψ is a tangle, but is not one of the orientations induced by V_1 or V_2 . Since τ is not induced by V_1 there is some $A \in \tau$ such that $|A^c \cap V_1| \geq |A \cap V_1|$. Choose this A such that $|A \cap V_1|$ is as small as possible; we will show that $|A \cap V_1| = 0$.

We are first going to show, that we may suppose without loss of generality that $A \cap V_2 = \emptyset$. So suppose for a contradiction that $A \cap V_2 \neq \emptyset$. It is easy to see that the costs of the cut $\{A^c \cup V_2, A \setminus V_2\}$ are at most the cost of the cut $\{A^c, A\}$. If τ contains $A \setminus V_2$ we could chose the cut $\{A^c \cup V_2, A \setminus V_2\}$ instead of $\{A^c, A\}$, so suppose that τ contains $A^c \cup V_2$.

As the costs of the cut $\{A \cap V_2, A^c \cup V_1\}$ are again at most the costs of $\{A, A^c\}$, our tangle needs to contain either $A \cap V_2$ or $A^c \cup V_1$. However the latter is not possible as $(A^c \cup V_1) \cap (A^c \cup V_2)A = \emptyset$ contradicting the consistency of τ . Thus $A \cap V_2 \in \tau$ which already verifies that τ contains a set disjoint from V_1 .

So we may assume that $A \cap V_2 = \emptyset$. Suppose that there is some $v \in A \cap V_1$ and consider the cut $\{A^c \cup \{v\}, A \setminus \{v\}\}$. Since $p \geq 2q$ it is straightforward to check that the cost of this cut is, as $A \subseteq V_1$, strictly lower than that of $\{A, A^c\}$. In particular its cost is less than Ψ , and hence τ contains an orientation of this cut. Since τ is a tangle with $a \geq 2$, and $A \cap (A^c \cup \{v\}) = \{v\}$, τ cannot contain $A^c \cup \{v\}$ and must therefore contain $A \setminus \{v\}$. However, $A \setminus \{v\}$ no contradicts the choice of A .

This shows that τ contains an A disjoint from V_1 . By a similar argument τ contains an B disjoint from V_2 . But now $A \cap B = \emptyset$ which contradicts the assertion that τ is a tangle. \square

Corollary 18 (Tangles equal blocks). *If $p > 3qn/(n - 2a)$ and*

$$q \frac{n^2}{4} < \Psi \leq \frac{n^2}{4} p \left(\frac{1}{3}(1+r-x)(1+r) - \left(\frac{1+r-x}{3}\right)^2 \right),$$

then, for \mathcal{P}_Ψ the set of all cuts of cost at most Ψ , there are precisely two \mathcal{P}_Ψ -tangles: τ_Ψ^1, τ_Ψ^2 . These correspond to V_1 and V_2 .

C.3 Necessary gap condition

For this part we need to introduce the concept of locally minimal cuts. A cut $\{A, A^c\} \in \mathcal{P}$ is a *local minimum* if moving any single $v \in V$ to the other side does not decrease the cost.

In generality for tangles for $a \geq 2$ every cut which is of minimum cost such that a given pair of tangles disagrees on it is a local minimum: If a \mathcal{P}_Ψ -tangle τ includes some A and some $A \setminus \{v\}$ is also in \mathcal{P}_Ψ then $A \setminus \{v\} \in \tau$, since the other orientation of $A \setminus \{v\}$ gives an inconsistency, $|(A \setminus \{v\})^c \cap A| = |\{v\}| = 1$. Similarly, any tangle that includes A^c then also includes $A^c \cup \{v\}$.

Lemma 19 (Local minimum cuts do not cut through the blocks). *Independently of the choice of parameters, as long as $p > 0$, every local minimum cut respects the blocks, that is if $\{A, A^c\}$ is a local minimum cut, then for $i = 1, 2$ either $V_i \subseteq A$ or $V_i \subseteq A^c$.*

Proof. Suppose for a contradiction that the contrary is true, i.e. that $\{A, A^c\}$ is a local minimum cut but that, without loss of generality, both $V_1 \cap A$ and $V_1 \cap A^c$ are non-empty. Pick some arbitrary $v \in V_1 \cap A$ and $v' \in V_1 \cap A^c$.

Since $\{A, A^c\}$ is locally minimal, the cut $\{A \setminus \{v\}, A^c \cup \{v\}\}$ has at least the cost of $\{A, A^c\}$, hence, as $w(v, v) = w(v', v') = 0$, we have

$$\sum_{x \in A} w(v, x) \geq \sum_{x \in A^c} w(v, x).$$

Similarly,

$$\sum_{x \in A} w(v', x) \leq \sum_{x \in A^c} w(v', x).$$

However, since v, v' both lie in V_1 , we have that $w(v, x) = w(v', x)$ for all $x \neq v, v'$, thus:

$$\begin{aligned} \sum_{x \in A} w(v, x) &\geq \sum_{x \in A^c} w(v, x) \\ &= \sum_{x \in A^c} w(v', x) + w(v, v') \\ &\geq \sum_{x \in A} w(v', x) + w(v, v') \\ &\geq \sum_{x \in A} w(v, x) + 2w(v, v') \end{aligned}$$

Which is a contradiction as, $w(v, v') = p > 0$. \square

Theorem 20 (No distinct tangles). *If $p < 2q$ and $a \geq 2$ then, for every Ψ and \mathcal{P}_Ψ the set of all cuts of cost at most Ψ , there is at most one \mathcal{P}_Ψ -tangle. In particular, there is no Ψ such that V_1 and V_2 induce distinct tangles.*

Proof. Suppose that there are two tangles. Then there exist a lowest cost cut on which they disagree. This cut is a local minimum since $a \geq 2$. By Lemma 19 the only local minimum cuts are $\{\emptyset, V\}$ and $\{V_1, V_2\}$. So the cut in question must be $\{V_1, V_2\}$.

Since this cut has cost $qn^2/4$, our two tangles have to be \mathcal{P}_Ψ -tangles for some $\Psi \geq qn^2/4$.

Let τ be the tangle with $V_1 \in \tau$. Pick any two disjoint $X_1, X_2 \subseteq V_1$ with $|X_1| = |X_2| = \lfloor |V_1|/2 \rfloor$. The cost of the corresponding cuts is

$$c(\{X_1, X_1^c\}) = c(\{X_2, X_2^c\}) = p \left\lfloor \frac{n}{4} \right\rfloor \left\lceil \frac{n}{4} \right\rceil + q \left\lfloor \frac{n}{4} \right\rfloor \frac{n}{2} \leq p \frac{n^2}{16} + q \frac{n^2}{8} \leq q \frac{n^2}{4}.$$

So τ contains one of each X_1 or X_1^c and X_2 or X_2^c . Take note that $|V_1 \cap X_1^c \cap X_2^c| \leq 1 < a$, so since τ is a tangle it cannot contain both X_1^c and X_2^c .

Without loss of generality let us assume that $X_1 \in \tau$. Let $X'_1 \subseteq X_1$ be of minimum size such that $X'_1 \in \tau$. Now for any $x \in X'_1$ observe that the cut $\{X'_1 \setminus \{x\}, (X'_1 \setminus \{x\})^c\}$ has lower cost than $\{X'_1, X_1^c\}$. Thus by the minimal choice of X'_1 the complement $(X'_1 \setminus \{x\})^c$ is in τ , but

$$|(X'_1 \setminus \{x\})^c \cap X'_1| = |\{x\}| = 1 < a,$$

which contradicts our assumption that τ is a tangle. \square

C.4 Identifying tangles from random cuts is hard

Note that all our results for this model rely on the fact that \mathcal{P}_Ψ contains *all* cuts of G up to cost Ψ rather than just a sample of those cuts. In practice \mathcal{P}_Ψ might consist of many cuts, and so one usually would try to perform some sampling strategy to obtain a ‘sensible’ subset of these cuts. The following result shows that sampling from \mathcal{P}_Ψ **uniformly at random is not a valid sampling strategy** for this purpose, as one would still be required to draw a sample of size exponential in n .

Observe that by Theorem 4 the blocks define \mathcal{P}_Ψ -tangles for *any* collection \mathcal{P} of cuts. Thus, in order for the two blocks to define distinct tangles it suffices for the sampled set of cuts to contain a single cut which *distinguishes* them – that is one cut $\{A, A^c\}$ such that more than half of V_1 lies in A and more than half of V_2 lies in A^c . Unfortunately, the number of these *good* cuts is exponentially small compared to the number of cuts up to any given cost Ψ :

Theorem 21 (Number of silly cuts). *Let p, q be fixed and let Ψ, a be chosen dependent on n such that the orientations induced by the blocks are distinct \mathcal{P}_Ψ -tangles for \mathcal{P}_Ψ the set of all cuts up to cost Ψ , then asymptotically the number of cuts not distinguishing these tangles is exponentially larger than the number of cuts distinguishing those tangles, for n going to infinity.*

This theorem implies that, if sampling cuts from \mathcal{P}_Ψ uniformly at random, one would need to sample exponentially many of the cuts in order for the two blocks to define distinct tangles, since our sample needs to include one cut for this which distinguishes the blocks. We will use the remainder of this section to prove the theorem.

We can construct all good partitions $\{A, A^c\}$ as follows: Starting with the partition $\{V_1, V_2\}$, we pick any subsets $G_1 \subseteq V_1$ of size $g_1|V_1| < |V_1|/2$ and $G_2 \subseteq V_2$ of size $g_2|V_2| < |V_2|/2$ and let $\{A, A^c\} = \{(V_1 \setminus G_1) \cup G_2, (V_2 \setminus G_2) \cup G_1\}$.

We observe that the cost of $\{A, A^c\}$ depends only on g_1 and g_2 . For fixed g_1 and g_2 there are exactly $\binom{|V_1|}{g_1 n} \cdot \binom{|V_2|}{g_2 n}$ many distinct cuts realizing this g_1 and g_2 . In this case we say that the good cut $\{A, A^c\}$ *corresponds to* (g_1, g_2) .

Similarly, we can construct all bad partitions $\{C, C^c\}$ as follows: Starting with the partition $\{\emptyset, V_1 \cup V_2\}$, we pick subsets $B_1 \subseteq V_1$ of size $b_1|V_1| < |V_1|/2$ and $B_2 \subseteq V_2$ of size $b_2|V_2| < |V_2|/2$ and let $\{C, C^c\} = \{B_1 \cup B_2, (V_1 \cup V_2) \setminus (B_1 \cup B_2)\}$. We observe that again, the cost of $\{C, C^c\}$ depends only on b_1 and b_2 . Moreover for fixed b_1 and b_2 there are exactly $\binom{|V_1|}{b_1 n} \cdot \binom{|V_2|}{b_2 n}$ many distinct cuts realizing this b_1 and b_2 . In this case we say that the bad cut $\{C, C^c\}$ *corresponds to* (b_1, b_2) .

Therefore if we can show that for $b_1 = g_1 < 1/2$ and $b_2 = g_2 < 1/2$ the cost of $\{A, A^c\}$ as constructed above is always as least as big as the cost of $\{C, C^c\}$, this would imply that there are at least as many bad partitions as good ones, since we can construct an injective function from the set of good into the set of bad partitions of cost $< k$. The cost of a bad cut for b_1, b_2 is

$$\frac{n^2}{4} (p(b_1 - b_1^2 + b_2 - b_2^2) + q(b_1 + b_2 - 2b_1 b_2))$$

and the cost of a good cut for g_1 and g_2 is

$$\begin{aligned} & \frac{n^2}{4} (p(g_1 - g_1^2 + (1 - g_2) - (1 - g_2)^2) + q(g_1 + (1 - g_2) - 2g_1(1 - g_2))) \\ &= \frac{n^2}{4} (p(g_1 - g_1^2 + g_2 - g_2^2) + q(1 - g_1 - g_2 + 2g_1g_2)) . \end{aligned}$$

However, for $b_1, b_2 < 1/2$ we have that

$$2b_1 + 2b_2 - 4b_1b_2 < 1$$

and thus

$$b_1 + b_2 - 2b_1b_2 < 1 - b_1 - b_2 + 2b_1b_2 ,$$

i.e. for $g_1 = b_1$ and $g_2 = b_2$ the cost of $\{C, C^c\}$ is indeed at most the cost of $\{A, A^c\}$. Therefore up to any given cost there are at least as many bad cuts as there are good ones.

Moreover, we can show a little bit more: For $\delta = 1 + q/p$ we can show that, under the condition that the cost of a good cut corresponding to (g_1, g_2) is at most $p \left(2 \left(1 + \frac{q}{p}\right)^2 / 9\right)$ (for larger Ψ , τ_k^1 is not a tangle by Lemma 14), then also the cost of a bad cut corresponding to $(\delta g_1, \delta g_2)$ is at most the cost of a good cut corresponding to (g_1, g_2) . Thus in this case we have, given a fixed Ψ and the set A_Ψ of all pairs (g_1, g_2) for which the cost of a good cut corresponding to (g_1, g_2) is at most Ψ , that there are exactly

$$\sum_{\substack{(i,j) \\ \binom{i}{|V_1|}, \binom{j}{|V_2|} \in A_\Psi}} \binom{|V_1|}{i} \cdot \binom{|V_2|}{j}$$

good cuts. However, there are at least

$$\sum_{\substack{(i,j) \\ \binom{i}{\delta|V_1|}, \binom{j}{\delta|V_2|} \in A_\Psi}} \binom{|V_1|}{i} \cdot \binom{|V_2|}{j}$$

bad cuts. Using these numbers it can be shown that for fixed $\delta > 1$ the number of bad cuts grows exponentially faster than then number of good cuts, as n goes to infinity.

C.5 Asymmetric block sizes

In the previous sections we analyzed the expectation case of the stochastic block model for two blocks of size $n/2$. In this section, we will consider the asymmetric case: one small block of size n_2 and one larger one of size $n_1 = rn_2$, where $r \geq 1$.

The calculations in the asymmetric case for the smaller of the two blocks are fairly similar to the symmetric one, except that some instances of r may appear in the calculations. Our strategy for finding the range of Ψ -values for which the blocks define tangles, and distinct ones at that, will be the same.

Suppose that V_2 is the smaller block, i.e. that $|V_1| = n_1 = rn_2$ and $|V_2| = n_2$. If the smaller block defines a tangle so will the larger block, so we will focus our efforts on the orientation defined by V_2 .

Let us first find the minimum cost of a cut that distinguishes the two blocks. The cost of the cut (V_1, V_2) works out to $n_2^2 r q$, and hence the blocks will define distinct orientations once $k > n_2^2 r q$. For $r = 1$ this is the same bound as before. Under the assumption that $p > 2r q$ (which we will make below) this cut is also still of the lowest cost among all cuts that distinguish the blocks.

As for the maximum value of Ψ for which the blocks define tangles we need two ingredients: Lemma 13 and Lemma 14. In the first of these we have some cut (A, A^c) such that A contains some fraction $\alpha < 1/2$ of V_2 , and we wish to move all of V_1 to either A or A^c . Running the same calculations as in Lemma 13 reveals that we can move all of V_1 to A without decreasing the cost of the cut if A already contains at least a fraction of $q(1 - 2\alpha)/(pr)$ of V_1 . Likewise we can move the block V_1 entirely into A^c once A^c contains a fraction $q(1 - 2\alpha)/(pr)$ of V_1 . These bounds generalize the symmetric case: for $r = 1$ they coincide with Lemma 13. In fact for $r > 1$ it only becomes easier to move V_1 around. In Lemma 14 we computed the minimum possible cost of a forbidden triple in the orientation induced by V_2 , assuming that the triples come in the shape produced by Lemma 13. Here the computations work as follows:

Suppose that (A, A^c) , (B, B^c) , and (C, C^c) are such that A, B^c , and C^c each contain V_1 , that B and C both contain some α -fraction of V_2 , and that A contains some $(1 - 2\alpha)$ -fraction of V_2 , where $\alpha < 1/2$. (This is the case $x = 0$ from Lemma 14.) Then we have

$$|B, B^c| = |C, C^c| = \alpha n_2^2 (r q + p(1 - \alpha))$$

and

$$|A, A^c| = 2\alpha n_2^2 (rq + p(1 - 2\alpha)).$$

These two terms are equal if $\alpha = (1 + rq/p)/3$. Plugging in that $\alpha < 1/2$ we obtain the bound

$$p > 2rq,$$

which for $r = 1$ matches the requirements of the symmetric case. From there the optimization argument works in exactly the same way.

D Pseudocode

In this section, we present the pseudocode for the algorithms used to compute and post-process tangles.

D.1 Finding tangles

As we described in Section 4 the strategy that we deploy to find all the tangles for a given family of cuts \mathcal{P} is a breadth-first traversal tree, see Figure 6b for an example of a complete output. In this tree each node represent a tangle τ and each leaf that we marked as maximal represent a tangle that cannot be extended anymore with the set of cuts at our disposal.

In Algorithm 1 we present the main loop for this algorithm. Supposed we are given an agreement parameter a and family of cuts $\mathcal{P} = \{P_i = \{A_i, A_i^c\}\}_i$ each of which has cost $\Psi_i \in \mathbb{R}$. We order \mathcal{P} according to their cost Ψ_i and then we iteratively try to add all the cuts. We terminate when either we cannot add a cut or when we run out of cuts.

Algorithm 1 finding_tangles

Require: Family of cuts $\mathcal{P} = \{P_i = \{A_i, A_i^c\}\}_i$ with cost Ψ_i and agreement parameter a
order \mathcal{P} with respect to Ψ_i
tangles = Tree()
for all $P_i \in \mathcal{P}$
 for all τ in non maximal leaves of tangles
 $\tau, \text{extended} = \text{add_cut}(\tau, P, a)$
 if not extended
 mark τ as maximal
 if all the leaves are maximal
 return tangles
Mark all the leaves as maximal
return tangles

In Algorithm 2 for each tangle τ that we have identified as non maximal we try to add both orientations of a new cut P to τ . Each orientation produce a potential new tangle τ' . We now need to check if τ' is consistent. The consistency of τ' can be checked by checking the consistency of the *core* of τ' , i.e. the set of all the inclusion minimal cuts in τ' . This is sufficient as if we have A, A', B, C such that $A' \subseteq A$, then

$$|A' \cap B \cap C| \geq a \implies |A \cap B \cap C| \geq a \quad (2)$$

Therefore if the core of a tangle is consistent so is the tangle. If τ' is consistent then we add it as a left or right child in the tree. Which side depends on the orientation that created τ' , left for A and right for A^c . Subsequent we mark that it was possible to extended τ . If neither orientation can be added we return that τ cannot be extended.

Algorithm 2 add_cut_to_tangle

Require: tangle τ , new cut $P = (A, A^c)$, agreement parameter a
extended = False
 $\tau' = \text{add_orientation_to_tangle}(\tau, A)$
if core(τ') is consistent for a
 $\tau.\text{add_left_child}(\tau')$
 extended = True
 $\tau' = \text{add_orientation_to_tangle}(\tau, A^c)$
if core(τ') is consistent for a
 $\tau.\text{add_right_child}(\tau')$
 extended = True
return $\tau, \text{extended}$

In Algorithm 3 we show how to add a new orientation A to a tangle τ . To do so we first add A to the specification of τ and then we update the core of τ if it is necessary.

Algorithm 3 add_orientation_to_tangle

Require: tangle τ , new orientation A
 add A to specification(τ)
for C in core(τ)
 if $C \subseteq A$
 return τ
 if $A \subset C$
 remove C from core(τ)
 add A to core(τ)
return τ

D.2 Post-processing to dendrograms

The output of Algorithm 1 is a tangle search tree, which reveals the cluster structure of a data set from the cut point of view. However, since traditional clustering objectives are concerned with assigning individual objects to clusters, we need to post-process the tangle search tree into an object point of view. To this end, we propose a procedure that builds on the hierarchical nature of the tangle search tree to convert it into a “soft dendrogram”.

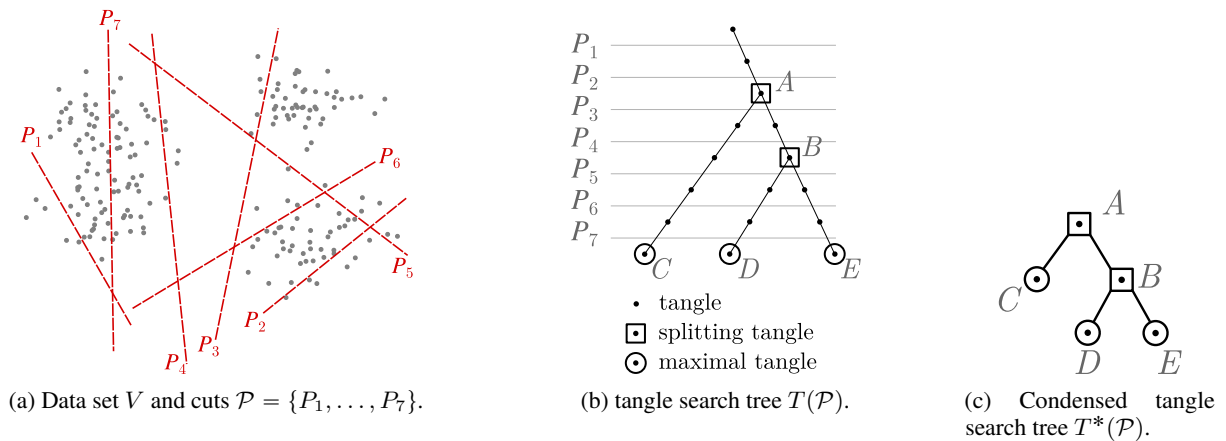


Figure 6: Example of tangles for a data set in \mathbb{R}^2 .

For a given set of partitions $\mathcal{P} = \{P_1, \dots, P_m\}$ sorted increasingly by their costs $c(P_i)$, let $T = T(\mathcal{P})$ be the corresponding tangle search tree obtained from Algorithm 1, see Figure 6a and 6b for an example. The tangle search tree is by construction a hierarchy on the cuts, which serves as a proxy for what we are eventually interested in, namely a hierarchy on the cluster structure of the objects. We extract this information from T based on the following intuition: when trying to add a cut P_i to a tangle τ , then either none, one, or both of its sides yield a consistent orientation. The first case implies that P_i cuts away too much of the structure that τ points to with respect to the previous cuts. These tangles τ are precisely the leaves of T and are called *maximal tangles*. Note that all tangles in T can be obtained by restricting maximal tangles to subsets $\{P_1, \dots, P_j\}$ of the cuts. In the second case, exactly one side of P_i can be consistently added to τ , and the resulting tangle points towards the same structure as τ . Lastly, a cut that yields consistent orientations for both sides subdivides the structure such that both smaller parts are large enough to contain clusters themselves. We then call τ a *splitting tangle*, because the next cut splits it into two different tangles. The splitting tangles are precisely the nodes of degree three in T . We employ this intuition by only considering the tangles that give insight into the hierarchical structure, which are the splitting and maximal tangles. That is, we restrict T to

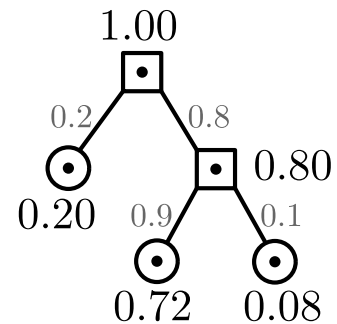


Figure 7: Tree T^* with node and edge attributes for a fixed object $v \in V$.

its nodes of degree three and leaves, then contract all paths between them. The resulting tree is denoted by T^* , an example is given in Figure 6c.

Like a dendrogram, the condensed tree T^* indicates how a data set separates into substructures, but it does not yet make a statement about which path a specific object takes at a splitting tangle. A naive approach would be to base this decision on the first cut after the splitting tangle, but this would waste all the clustering information given by similar cuts. Instead, we first identify the set of all cuts that distinguish between the subtrees of a splitting tangle τ . To do so, let $\tau^{(\text{left})}$ and $\tau^{(\text{right})}$ denote the subtrees at τ and define

$$\mathcal{P}(\tau) := \{P \in \mathcal{P} \mid P(\tau') \neq P(\tau'') \quad \forall \text{ leaves } \tau' \in \tau^{(\text{left})}, \text{ leaves } \tau'' \in \tau^{(\text{right})}\}. \quad (3)$$

In particular we require that every partition $P \in \mathcal{P}(\tau)$ is oriented by every tangle corresponding to a leaf below τ . This definition is equivalent to requiring that every tangle corresponding to a leaf in the one subtree orients P one way and every tangle corresponding to a leaf in the other subtree orients P the other way. In this sense, the cuts in $\mathcal{P}(\tau)$ are the ones that help in distinguishing between the subtrees of τ . In the example of Figure 6 for the splitting tangle τ at node A, we would have $\mathcal{P}(\tau) = \{P_3, P_4, P_7\}$. We can now use these cuts to decide whether an object $v \in V$ goes to the right subtree of τ (the left subtree is then implicit, so we focus on the right side). All cuts in $\mathcal{P}(\tau)$ serve the same purpose of subdividing τ , but not all of them are equally fundamental as measured by their costs $c(P)$, which we account for with a non-increasing function $h: \mathbb{R}_{\geq 0} \rightarrow \mathbb{R}_{\geq 0}$. Let $P^{(\text{right})} \in \mathcal{P}$ be the orientation of P in the right subtree of τ and define the probability that object v belongs to the right subtree of τ as

$$p_{\tau}^{(\text{right})}(v) = \frac{\sum_{P \in \{P \in \mathcal{P}(\tau) \mid v \in P^{(\text{right})}\}} h(c(P))}{\sum_{P \in \mathcal{P}(\tau)} h(c(P))}. \quad (4)$$

Using these vectors $p_{\tau}^{(\text{right})}$, we can describe the stochastic process of how an object v traverses the tree T^* . This can be converted to node attributes by computing the probability $p_t(v)$ that v arrives at node t as the product of the edge probabilities along the unique path from the root to τ , see Figure 7 for an example.

The final output of this post-processing approach is the attributed tree $(T^*, (p_t)_t)$, which is a “soft” version of a dendrogram. Since every node attribute $p_t \in [0, 1]^n$ consists of probabilities for every object, the tree can be visualized with heatmaps as done in Figure 2.

D.3 Conversion into flat clusterings

The soft dendrogram $(T^*, (p_t)_t)$ represents a hierarchical cluster structure, but can be converted naturally into a flat clustering as follows. We first fix a subset $\mathcal{T} \subseteq T^*$ with the property that every path from the root to a leaf contains exactly one node in \mathcal{T} , for example the set of all leaves. Formally, this describes the maximal antichains in T^* with respect to the tree-order. In terms of the heatmaps p_t , these are precisely the subset of nodes that satisfy $\sum_{t \in \mathcal{T}} p_t(v) = 1$ for every $v \in V$, which means that $(p_t)_{t \in \mathcal{T}}$ is a soft clustering of the data set. One way to obtain a corresponding hard clustering is the maximum-likelihood assignment of objects to clusters, that is, $\text{cluster}(v) = \text{argmax}_{t \in \mathcal{T}} p_t(v)$.

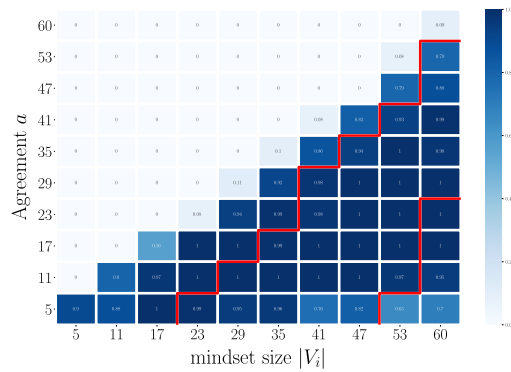
E Extra experiments: mindsets

In this section, we present additional experiments for the mindset scenario. We will roughly distinguish between “informative” cuts that separate clusters, making them useful for clustering, and “noisy” cuts that cut through a cluster, making them useless for clustering. Specifically for the mindset model, these cuts are given by questions: informative questions are the ones defined by the model, with a predefined groundtruth answer that is flipped with noise probability p . This is not to be confused with additional noise questions, which are by definition answered randomly by every person.

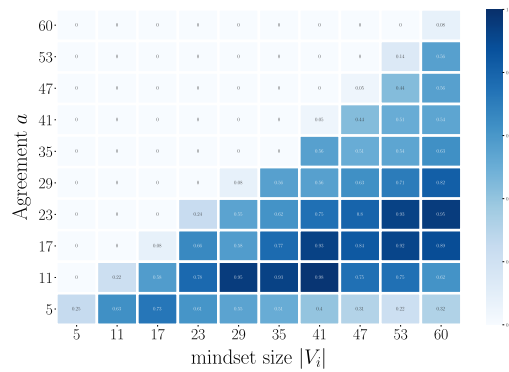
E.1 Choosing the agreement parameter a

In the mindset scenario, one important parameter to fix is the agreement parameter a that we have to choose for the tangle algorithm. From Theorem 3, given a level of noise p we have a theoretical upper and lower bound on the choice of a such that the discovered tangles can represent the mindsets.

In Figure 8 we observe that in practice, where we do not consider all possible cuts but just the ones induced by the questions, the choices of a that yield good results are even more than theory suggests. In Figure 8a with noise $p = 0.1$ the theoretical bounds are shown as red lines; $0.1 \cdot |V_2| < a < 0.35 \cdot |V_2|$. In Figure 8b with a noise level $p = 0.2$, theory suggests $0.2 \cdot |V_2| < a < 0.2 \cdot |V_2|$ yielding an empty interval. In both cases good results are achieved even for values of a outside the bounds. Based on experiments on different data sets, using an agreement parameter between $0.3n$ and $0.5n$ seemed to work in most cases.



(a) noise $p = 0.1$.



(b) noise $p = 0.2$.

Figure 8: Choice of agreement parameter a . Mindset model with $k = 2$ mindsets with different mindset sizes as on the x-axis for two different noise p as indicated in the subtitles. This model uses $m = 40$ informative questions and no additional noisy questions. Overall number of data points is twice the mindset size (thus, increasing along the x-axis). Tangles obtained using the m cuts induced from the questions and agreement parameter a as indicated on the y-axis. The values are the adjusted Rand index (darker is better; 0 for random guessing, 1 for perfect recovery). Values averaged over 10 runs. The red lines show the theoretical bound of Theorem 3 for $n \rightarrow \infty$.

E.2 Dealing with noisy cuts

We consider a cut to be “noisy” if it cuts through clusters rather than between clusters, which makes them less informative for clustering. An example for noisy cuts are random cuts, where every object randomly chooses a side. As discussed in Section 2.2, noisy cuts typically incur a high cost c , because they separate highly cohesive structures. This puts them last in the increasing sets \mathcal{P}_Ψ and in the tangle search tree, and therefore does not interfere with the noiseless, informative cuts. However, this imposes a problem for the post-processing: **up to which level does the tangle search tree still contain information?** In Section F.5 we emphasize that this problem concerns only the post-processing, not the tangles themselves.

A naive approach, for example the one we use in this paper (Section D.2), simply uses the whole tangle search tree and relies on the agreement parameter a to prevent noisy cuts from forming consistent orientations: by increasing a , an orientation of the cuts has to agree more strongly on a structure in order to form a tangle. Intuitively, orientations that include the noisy cuts become inconsistent first, because the noisy cuts only agree “by chance” on a small set of points. (Consider k random cuts. The intersection of all sides for a random orientation contains 2^{-k} objects on average, making $a < 2^{-k}$ unsuited in this case for excluding random cuts.) See Section 2.2 for a discussion of the agreement parameter. The downside of this approach is that **increasing a too much will eventually prevent the smallest ground-truth clusters from inducing consistent orientations**. This happens solely because of their size, even if there is not a single cut through this cluster.

A possible remedy broached in Section 5 is to address this problem directly in the post-processing by restricting the set of cuts, respectively the tangle search tree, to the ones of cost less than some Ψ_{\max} . The idea is that there should be a **notable gap between the cost of informative and noisy questions**, which allows to filter out the noisy questions in this way. The example in Figure 9 illustrates this for the mindset model with 2 mindsets, 40 informative questions and an additional 20 noise questions. Compared to considering all questions as in Figure 9a, Figure 9b shows that we can increase the performance by removing the high-cost cuts for reasonably small model noise p .

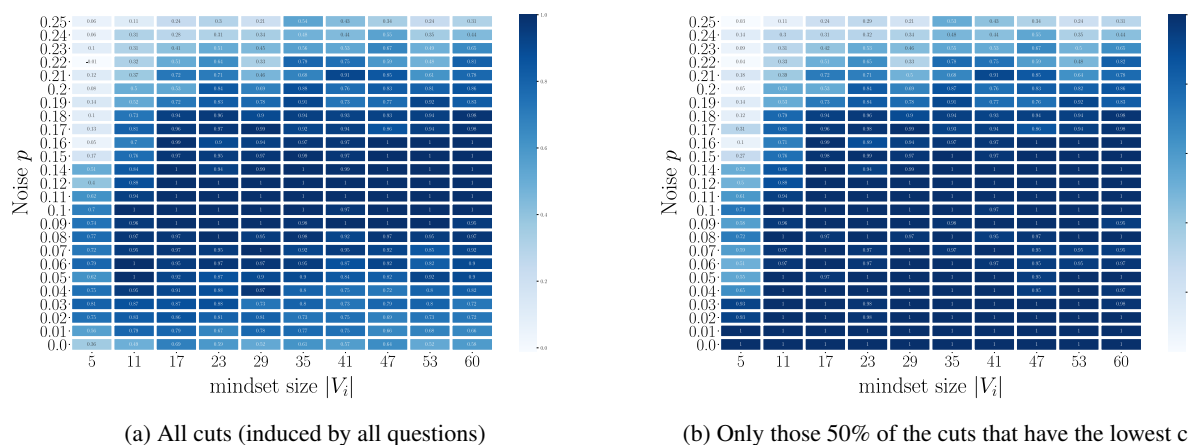


Figure 9: Does dropping the cuts of highest cost help with recovery? Mindset model with $k = 2$ mindsets with different mindset sizes as on the x-axis and noise level p as on the y-axis. This model uses $m = 40$ informative questions and 20 additional noisy questions (answers are random). Overall number of data points is twice the mindset size (thus, increasing along the x-axis). Tangles obtained using all or a percentage the cuts induced from the features, as indicated in the subtitle, and agreement parameter a equal to $1/3$ of the mindset size (thus, increasing along the x-axis). The values are the adjusted Rand index (darker is better; 0 for random guessing, 1 for perfect recovery). Values averaged over 10 runs.

It should be noted that this problem of dealing with noisy cuts does not appear in theory when considering $\mathcal{P} = \{\text{all possible cuts}\}$. This is because as we increase the cost Ψ , the cuts in \mathcal{P}_Ψ separate increasingly large portions of a cluster. By the time this cut is large enough such that its smaller side contains more than a objects, the many other cuts already included in \mathcal{P}_Ψ prevent an orientation towards the smaller side. Therefore, **only a gap between informative and noisy cuts allows the noisy cuts to be oriented consistently**, that is, to produce “false positives”. The negative consequences of this gap can be mitigated by the post-processing, but they can only be prevented by the pre-processing, that is, the cut finding strategy.

E.3 Interplay between a , Ψ_{\max} , and noisy cuts

After establishing that it is sensible to consider Ψ_{\max} , we now turn back to the agreement parameter a . Both parameters Ψ_{\max} and a attempt to remove the influence of noisy cuts in different ways, but how do they interact? Figure 10 shows this interplay for the mindset model with three mindsets of unequal sizes, 10 informative questions, and 5 noise questions. There are several interesting phenomena observable in this figure.

For a fixed a , we can observe that increasing the percentile of questions eventually causes the adjusted Rand index to plateau. This is because adding cuts to the algorithm will only cause the tangle search tree to grow as long as there are still consistent orientations. Once no consistent orientations exist anymore, the tree will remain unchanged, and so will any further post-processing. How early the plateau is reached depends on a : the larger a , the harder it is to satisfy the consistency condition, and the earlier the plateau is reached. If a is small enough, it might not be reached at all. Another effect of increasing the percentile is that the performance first increases, as we include more informative questions, but starts to decrease once we start including noise questions at about $2/3$, which is the fraction of informative questions.

Reversely, if we fix a percentile and look at different a , we can observe a general trend: first, the performance improves up to $a = 30$ or $a = 40$, and then starts to decrease again. This reflects the theoretical discussion at the beginning of this section about increasing a to remove noisy cuts: the initial increase in performance is because noisy cuts become harder to orient consistently, which removes the corresponding nodes from the tangle search tree. As a gets larger than 50, the size of the smallest cluster, tangles cannot identify it anymore, which results in a loss of performance.

However, the takeaway of this figure is the interplay between a and Ψ_{\max} . **The optimal performance is achieved only by a joint effort of both parameters, and not by a alone.** Another advantage of tuning both parameters is that for a correctly chosen Ψ_{\max} that removes the noise questions (in this case a percentile less than $2/3$), the choice of a becomes less critical. This can be seen by considering the lines for $a = 30$ and $a = 40$, which follow a very similar trajectory up until the $2/3$ mark, then become significantly different.

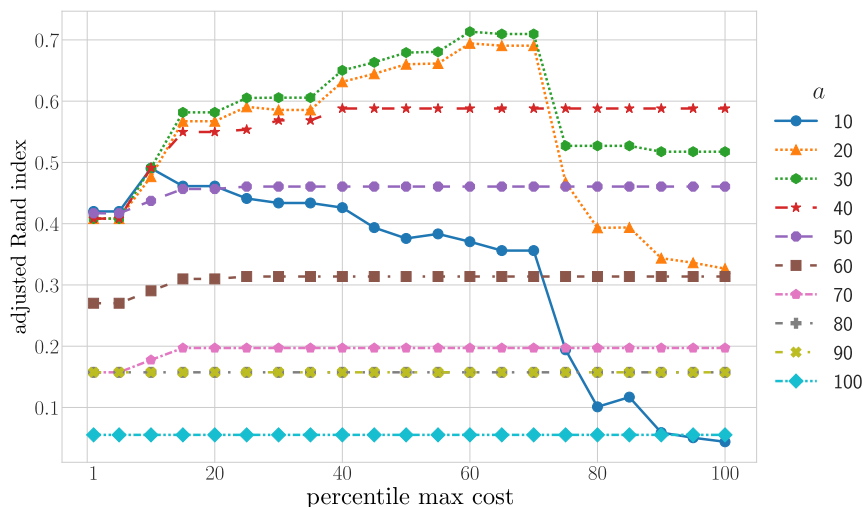


Figure 10: Interplay between agreement parameter a and maximal cost Ψ_{\max} . Mindset model with $k = 3$ mindsets, one with 100 two with 50 persons, and noise parameter $p = 0.1$. Overall number of data points is the 300. This model uses $m = 10$ informative questions and 50 additional noisy questions (answers are random). Tangles are obtained using only the top s -th percentile of the cuts induced by the questions, as specified on the x -axis in the plot. To compute the percentiles, cuts are ordered according to their costs; for example, the 10% percentile contains the 10% of the cuts with the lowest costs. Each line uses a different agreement parameter a . The values on the y -axis are the adjusted Rand index (darker is better; 0 for random guessing, 1 for perfect recovery). Values averaged over 10 runs.

E.4 How many cuts do we need?

Next we consider how many questions we have to ask in the mindset model so that we can recover the true mindsets for the points. In Figure 11 we try to recover the points of two mindsets, each of size 40, with $a = 13 \approx 40/3$. We see that the more noise we introduce the more questions we need for good recovery. Saturation is achieved quickly for all the noise levels. Increasing the number of points per mindsets would make them less prone to random errors, but then convergence would be fast due to the number of points and the effect of saturation with increasing number of questions would be less visible.

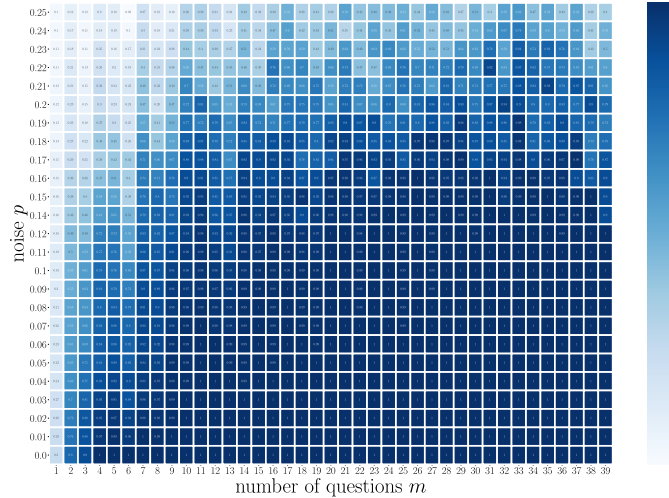


Figure 11: How many questions do we need? Mindset model with $k = 2$ mindsets with 40 persons each and noise p as on the y-axis. This model uses a number of informative questions as on the x-axis and no additional noisy questions. Overall number of data points is twice the mindset size. Tangles obtained using all or a percentage the cuts induced from the features and agreement parameter $a = 13$ equal to $1/3$ of the mindset size. The values are the adjusted Rand index (darker is better; 0 for random guessing, 1 for perfect recovery). Values averaged over 10 runs.

At this point we want to point out the difference between the tangles representing the true mindsets and the ability to actually recover the ground truth for all the points. Especially having less questions does not necessarily result in the tangles representing the mindsets worse and vice versa. For a small number of questions and some noise on the model, the tangles might still coincide with the mindsets but there might be points that are closer to another mindset than to their true label in terms of the similarity function. This, in turn, makes perfect assignment of the points impossible. Another effect is that increasing the number of questions makes the mindsets that we want to discover more complex and has a direct effect on the similarity between the points. Intuitively this could make discovery of the mindset more difficult while recovery of the points became easier.

E.5 Unbalanced mindsets are harder to recover

Our theoretic results in Section 3.1 have been proved in the case where we have balanced mindsets of equal size. In Figure 11 we explore what happens if this assumption is violated. We see that there is an immediate drop in the quality of the reconstruction as soon as the assumption is violated but the quality does not decline dramatically until we pass the point where one cluster is half of the other. To be able to get consistent orientations of the cuts pointing towards the smaller clusters, we need to adapt our agreement accordingly. The smaller our agreement parameter gets the more likely it is that the large cluster gets split into two, or more, small clusters, resulting in worse recovery. Nevertheless the true large cluster very likely will be represented in the hierarchical structure of the tangle search tree. More insights regarding this is discussed in Supplement F.5.

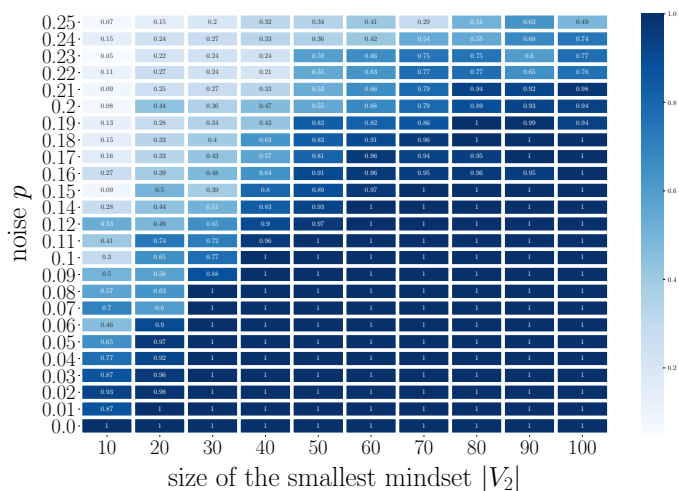


Figure 12: Effect of unbalanced cluster sizes. Mindset model with $k = 2$ mindsets: one mindset of 100 persons and one mindset of size as indicated on the x-axis. Noise p as on the y-axis. The overall number of data points is the sum of the two mindsets sizes (thus, increasing along the x-axis). Tangles obtained using all or a percentage the cuts induced from the questions, and agreement parameter a equal to a third of the smallest mindset size (thus, increasing along the x-axis). The values are the adjusted Rand index (darker is better; 0 for random guessing, 1 for perfect recovery). Values averaged over 10 runs.

F Extra experiments: stochastic block model

In the following we present additional experiments for graphs sampled from the stochastic block model. Aside from the fact that cuts need to be generated in a pre-processing phase, rather than being naturally given, we mostly observe the same phenomena as for the mindset model in Section E.

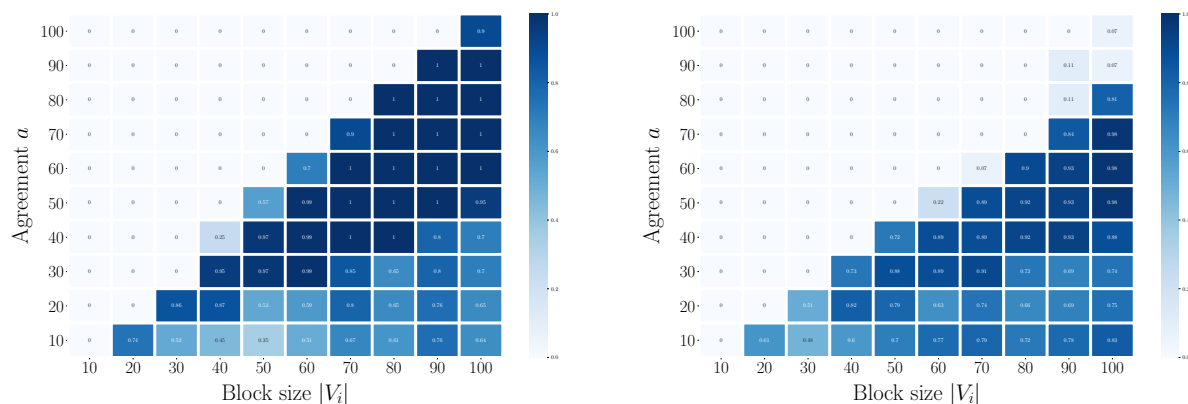
F.1 Algorithm to find initial cuts in the pre-processing phase

In the graph clustering setting, where we do not have naturally given cuts, the pre-processing step of generating these is an important part of the algorithm. Along the way we experimented with several algorithms to generate the initial cuts. From Supplement C.4 we know that using completely random cuts is not a viable strategy. Besides randomized algorithms such as Karger’s algorithm (Karger, 1993) we also tried the coarsening-refinement approach used in METIS (Karypis and Kumar, 1998). In the end we settled for a version of the **Fiduccia-Mattheyses-Algorithm** (Fiduccia and Mattheyses, 1982), which is a local search heuristic for finding mincuts. We abbreviate it by FM in the following. The algorithm is based on the Kernighan-Lin-Algorithm presented in Kernighan and Lin (1970). Starting with an initial partitioning, in each iteration it greedily chooses the most promising node to switch partitions, tracking the gain of each move. In the end it performs the sequence of actions with the greatest improvement on the cost of the cut. The algorithm always converges to a local optimum, but can be early stopped to improve runtime while still returning sufficiently good cuts. In the original algorithm, an initial partition and a ratio parameter r is given. This parameter avoids primitive cuts, such as all points ending up on one side, by forcing the final partition to have a ratio of approximately r . Since in our application we do not know which ratio we should aim for, we adapted the algorithm, giving a lower bound parameter l

that forces the size of the smaller partition to contain at least $l\%$ of the points. If we happen to have prior knowledge on the size of the clusters, it considerably helps to choose the parameter l accordingly.

F.2 Rule of thumb for choosing the agreement parameter a

As a general rule of thumb, we discussed in Section 2.2 that a should be chosen slightly less than the size of the smallest cluster. Figure 13 shows the hard clustering performance of tangles as measured by the adjusted Rand index for two stochastic block models of different density with two equal-sized blocks for a variety of block sizes and agreement parameters. The general trend is that the optimal performance is achieved for a slightly below the block size. The performance decreases if a falls too much behind, which can be attributed to the presence of noisy cuts that form consistent orientations. If a is too large, the ground-truth blocks themselves cannot form consistent orientations, which prevents the algorithm from discovering them.



(a) within-group connectivity $p = 0.3$,
between-group connectivity $q = 0.1$

(b) within-group connectivity $p = 0.6$,
between-group connectivity $q = 0.4$

Figure 13: Choice of agreement parameter a . Stochastic block model with $k = 2$ clusters, cluster size as indicated on the x-axis, within-group and between-group connectivity as indicated in the subtitle. The overall number of data points is twice the cluster size (thus, increasing along the x-axis). Tangles obtained using all the cuts from 50 cuts computed with the FM algorithm with lower bound l set to 0.4 and agreement parameter a as indicated on the y-axis. The values are the adjusted Rand index (darker is better; 0 for random guessing, 1 for perfect recovery). Values averaged over 10 runs.

F.3 Noisy cuts

The problem of noisy cuts is not restricted to the mindset model, but can also be a nuisance for the stochastic block model. It might be even more relevant here, because the cuts need to be computed in a pre-processing step as discussed in Section F.1, which, depending on the algorithm used, can produce a large number of noisy cuts.

Similar to Figure 9, in which we discussed the impact of noise questions on the result in the mindset model, we now consider noisy cuts in the stochastic block model. Figure 14 shows experiments on the block model with two equal-sized blocks of 100 points for different edge probabilities p and q . The set of cuts is obtained by using the FM algorithm with different values for its lower bound l , where smaller values of the lower bound yield a larger number of noisy cuts. Without adapting the agreement parameter a or the upper bound for the costs Ψ_{\max} as discussed in Section E.2, we observe that the performance in the setting with more noisy cuts (Figure 14a) is worse than the less noisy setting (Figure 14b). In Section 5, we discussed that a set of good cuts in combination with an appropriate agreement parameter can yield results that are better than our theoretical bound (Figure 4b). On the other hand, a bad set of cuts as in the noisy setting of Figure 14a can also do worse than the bound. This is because the bound is based on the set of all possible cuts, and therefore serves only as a proxy for the practical setting.

F.4 Interplay between a , Ψ_{\max} , and noisy cuts

Given a set of cuts, we now look at the influence of a and Ψ_{\max} on the performance. A detailed discussion about the codependency of a and Ψ_{\max} can be found in Section E.3 where we investigate this for the mindset model. Contrary to

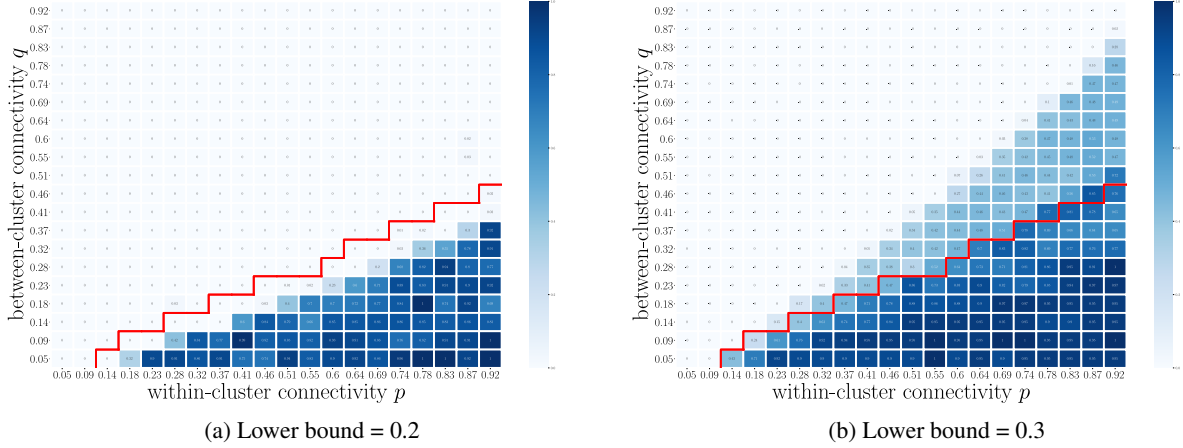


Figure 14: Effect of noisy cuts on the ability to recover. Stochastic block model with $k = 2$ clusters of size 100 point each, within-group connectivity p as indicated on the x-axis, between-group connectivity q as indicated on the y-axis. The overall number of data points is twice the cluster size. Tangles obtained using all the cuts from 50 cuts computed with the FM algorithm with lower bound l set as in subtitle and agreement parameter $a = 50$. The values are the adjusted Rand index (darker is better; 0 for random guessing, 1 for perfect recovery). Values averaged over 10 runs.

the mindset model, we have theoretical guidance for choosing a combination of a and Ψ_{\max} and refer to Theorem 3 for a more theoretical insight on this. In Figure 15 we can see that the best performances independent of a are achieved for a percentile of 20%. This indicates that our pre-processing algorithm yields a lot of noisy cuts which emphasizes the usefulness of setting Ψ_{\max} . Depending on the quality of the initial cuts, the amount of bad cuts might vary a lot — which once more reveals the importance of the pre-processing and that finding the optimal parameter settings is not trivial. The main conclusion we draw in Section E.3 can also be seen in this experiment for the stochastic block model. Both parameters are important, and we achieve best results by setting both.

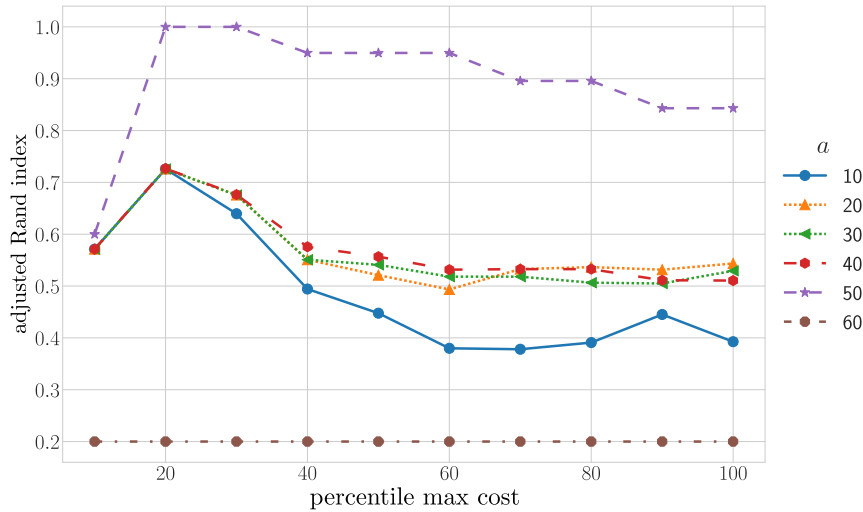


Figure 15: Interplay between agreement parameter a and maximal cost Ψ_{\max} . Stochastic block model with $k = 2$ clusters of size 100 point each, within-group connectivity $p = 0.3$ between-group connectivity $q = 0.1$. The overall number of data points is twice the cluster size. Tangles obtained using the only the top n -th percentile from 20 cuts computed with the FM algorithm with lower bound l set to 0.2. The percentile is specified on the x-axis. Each line uses a different agreement parameter a . The values on the y-axis are the adjusted Rand index (darker is better; 0 for random guessing, 1 for perfect recovery). Values averaged over 10 runs.

F.5 Tangle search tree contains all the information

In this set of experiments we want to point out that the tangle search tree contains a lot of information that might not always be used in our current post-processing approach.

To investigate the additional information generated by the tangle algorithm, we assume we know what we are looking for: we use the ground truth to determine which tangles represent it best, and then evaluate the most promising tangles. Given the initial cuts, we consider all tangles for every cost and calculate the adjusted Rand index for each of them. Then we select the tangle orienting only the cuts lower or equal to the cost that yields the best result. We call this approach “full tree” approach. Note that this approach is not applicable in practice, as we require to know the ground truth. This experiment only serves to highlight that the tangles in most cases offer all the information we need for recovery.

In Figure 16 we present the results of our post-processing presented in D.3 in comparison to the the “full tree” approach: on the left column we can see the output of our hard clustering post-processing described in Supplement D.2 and D.3, on the right column we can see the results when leveraging the information of the whole tree. We can see that there is more information in the whole tree than only in the leaves. **This stresses that there is still space for improvement in the post-processing algorithm and thus in the results we achieved so far.**

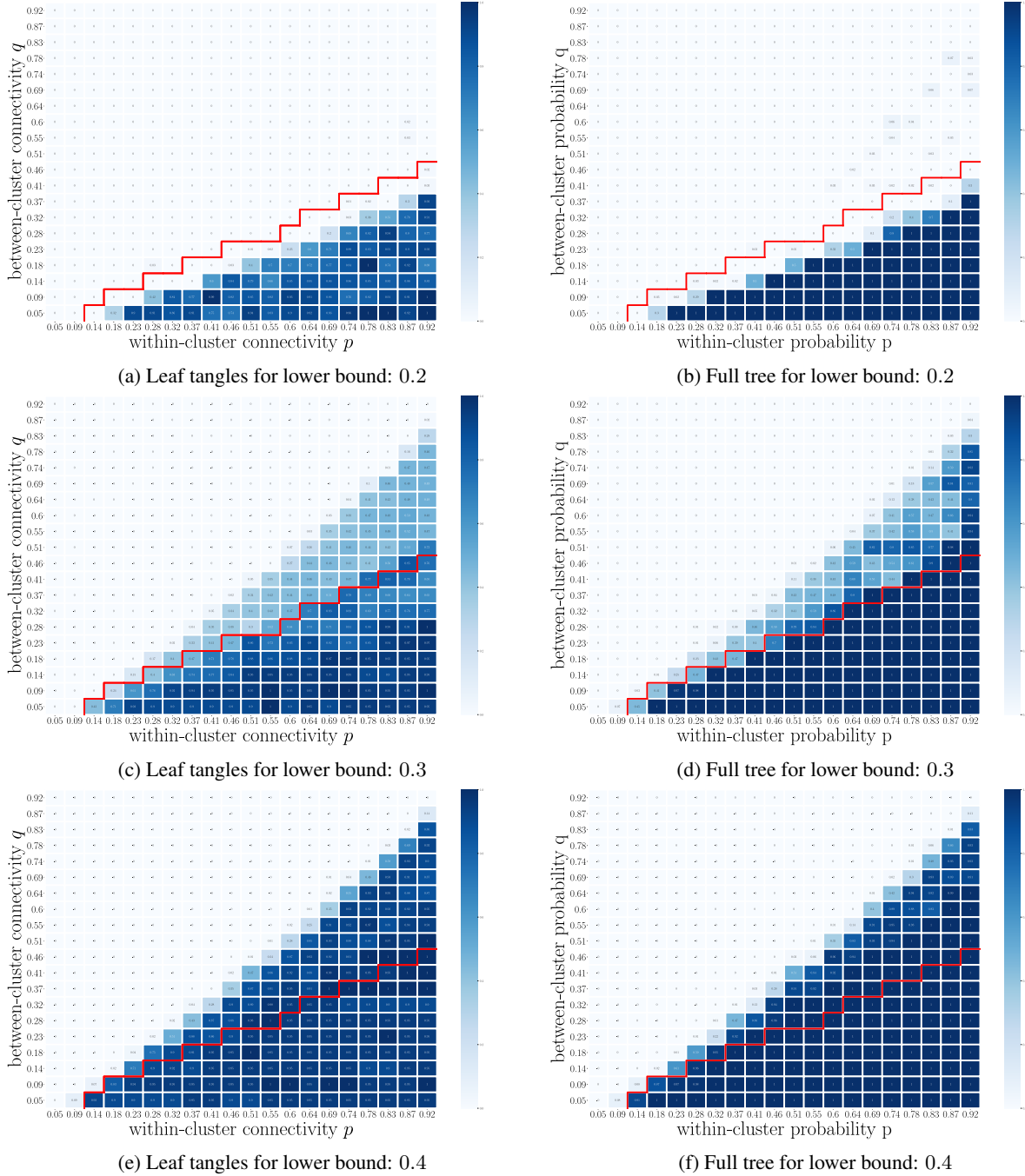


Figure 16: Difference between looking only at the clustering induced by the leaves or at the best clustering induced by the full search tree. Stochastic block model with $k = 2$ clusters of size 100 point each, within-group connectivity p as indicated on the x-axis, between-group connectivity q as indicated on the y-axis. The overall number of data points is 200. Tangles obtained using all the cuts from 50 cuts computed with the FM algorithm with lower bound l set as in subtitle and agreement parameter $a = 50$. The values are the adjusted Rand index (darker is better; 0 for random guessing, 1 for perfect recovery). The red lines show the theoretical bound of Theorem 5. Values averaged over 10 runs.

F.6 Tangles vs. spectral clustering

In Figure 17 we can see a set of experiments that compare the performance of the hard clustering post-processing of tangles to the one of spectral clustering on samples of the stochastic block model. We ran the spectral clustering algorithm provided by sklearn. This version implements the standard normalized spectral embedding algorithm using k-means for final classification into k clusters. We set the following parameters: number of clusters = 2, number of eigenvectors = 2 and number of initialization of k-means = 10. Tangles were computed with $a = 50$ and a lower bound in the FM algorithm of 0.4. The figure shows that tangles do not yet achieve as good reconstruction as spectral clustering. We discussed different phenomena in the previous section, and as we continue to further understand the interplay of parameters and the behavior of the algorithm on different data we do see room for improvement, especially in the pre- and post-processing of the algorithm. Note that the point of this paper is not to establish tangles as a state of the art clustering algorithm but to shed light on the possibilities they bring.

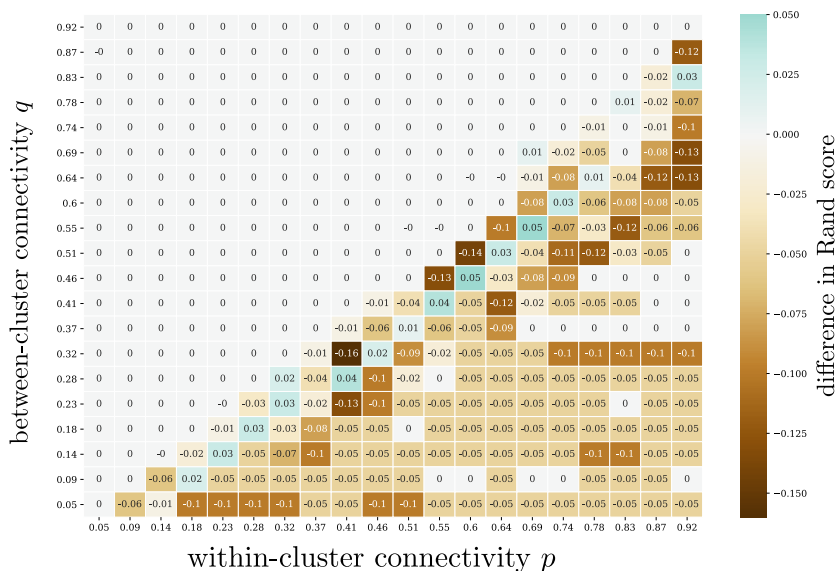
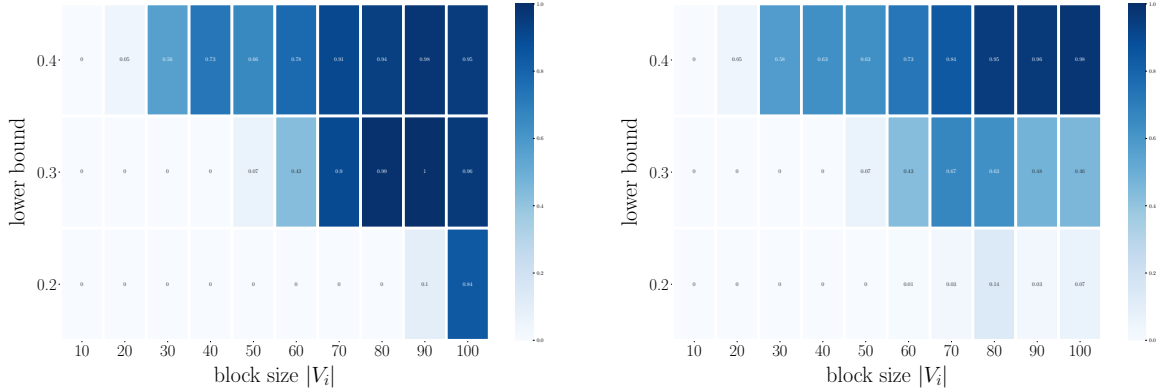


Figure 17: Comparison between the hard clustering produced by tangles and the hard clustering produced by spectral clustering. Stochastic block model with $k = 2$ clusters of size 100 point each, within-group connectivity p as indicated on the x-axis, between-group connectivity q as indicated on the y-axis. The overall number of data points is 200. Tangles obtained using all the cuts from 50 cuts computed with the FM algorithm with lower bound set as 0.4 and agreement parameter $a = 50$. Spectral clustering computed using number of clusters: 2, number of eigenvectors: 2 and number of initialization of k-means: 10. The values are differences in the adjusted Rand index (higher is better for tangles, lower for spectral clustering). Values averaged over 10 runs.

F.7 Unbalanced blocks are harder to recover

In this series of experiments we investigate the performance of the algorithm in the case of unbalanced blocks in a stochastic block model. In Figure 18a we do so in the case of a sparse graph (within-group connectivity $p = 0.1$ and between-group connectivity $q = 0.3$) and in Figure 18b for a more dense graph (within-group connectivity $p = 0.6$ and between-group connectivity $q = 0.4$). We set a to half of the size of the smaller cluster and do not tune Ψ_{\max} , so use all the cuts we find.

As with mindsets we see that once that the blocks start to be unbalanced recovering them becomes much harder. For a discussion on this we refer to Supplement E.5.



(a) within-group connectivity $p = 0.3$, between-group connectivity $q = 0.1$ (b) within-group connectivity $p = 0.6$, between-group connectivity $q = 0.4$

Figure 18: Effect of unbalanced cluster sizes. Stochastic block model with $k = 2$ clusters, one cluster of size 100 and one cluster of size as indicated on the x-axis, within-group and between-group connectivity as indicated in the subtitle. The overall number of data points is the sum of the cluster sizes (thus, increasing along the x-axis). Tangles obtained using all the cuts from 50 cuts computed with the FM algorithm with lower bound set as on the y-axis and agreement parameter a equal to half of the smallest cluster size (thus, increasing along the x-axis). The values are the adjusted Rand index (darker is better; 0 for random guessing, 1 for perfect recovery). Values averaged over 10 runs.

G Soft clustering for more data sets

In this section, we present some additional soft clustering outputs produced by our algorithm. In the paper we mostly stressed the hard clustering scenario as it is the most interpretable and directly connected to the theory but we believe that soft clustering is an area where tangles can truly help the community. In plot 19 we see how the soft clustering can work really well on a real world data set like the Breast Cancer Wisconsin data set. The data set was plotted in two dimensions with t-SNE. As such we should refrain from giving any geometric interpretation, but with this caveat in mind we can see that the algorithm is capable of capturing the uncertainty near the class boundary. This would allow an expert to use their domain knowledge to properly assign a difficult point to a specific cluster.

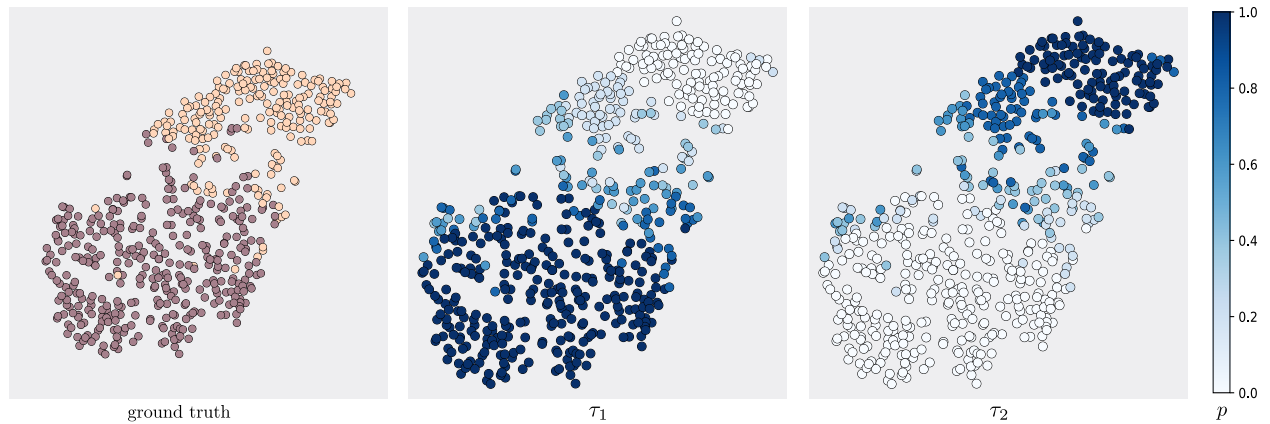


Figure 19: Output of the soft clustering post-process for the Breast Cancer Wisconsin data set

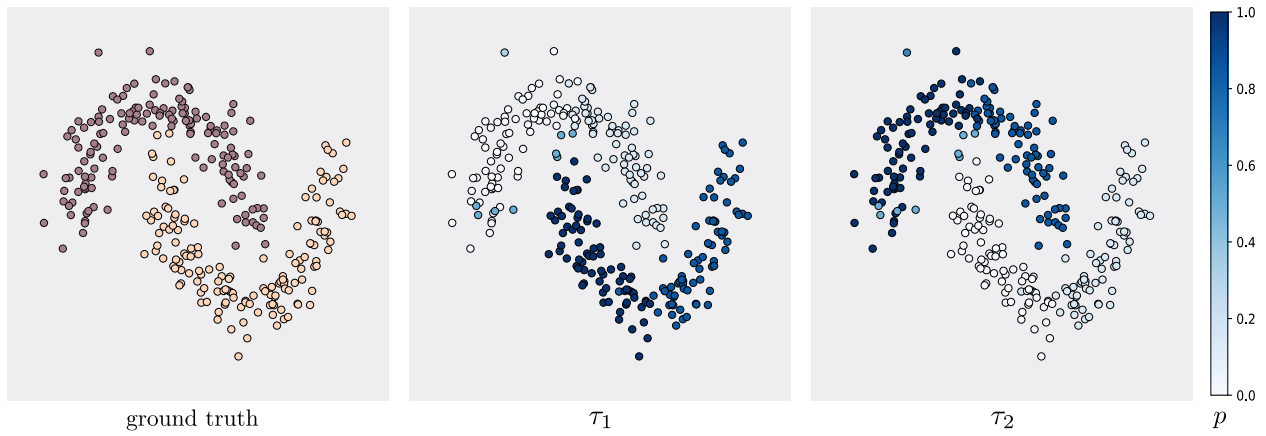


Figure 20: Output of the soft clustering post-process for a half moons data set

In Figure 22 we present the output for the soft clustering for a mixture of 4 standard Gaussians in Figure 21. We can see that the soft clustering output is more informative than the hard clustering one. As before we see that the algorithm detects the uncertainty near the class boundaries and it highlight such uncertainty in the output.

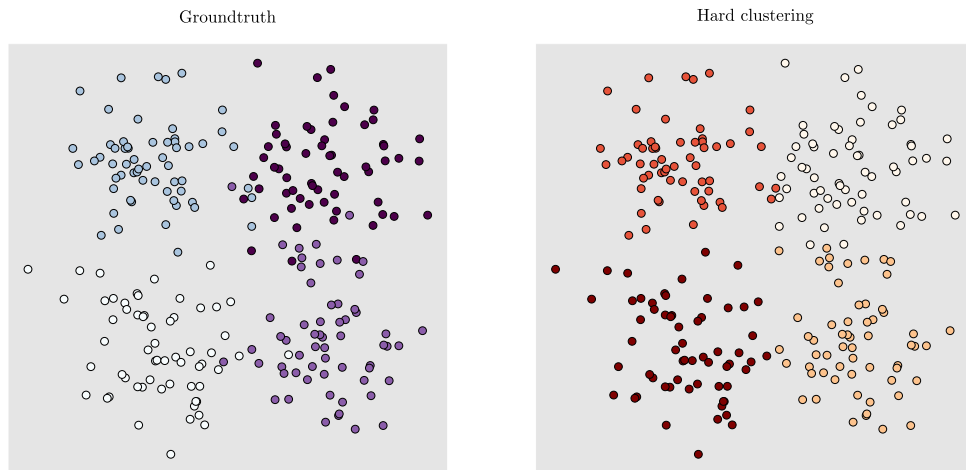


Figure 21: Groundtruth and hard clustering post-process for a mixture of four gaussians.

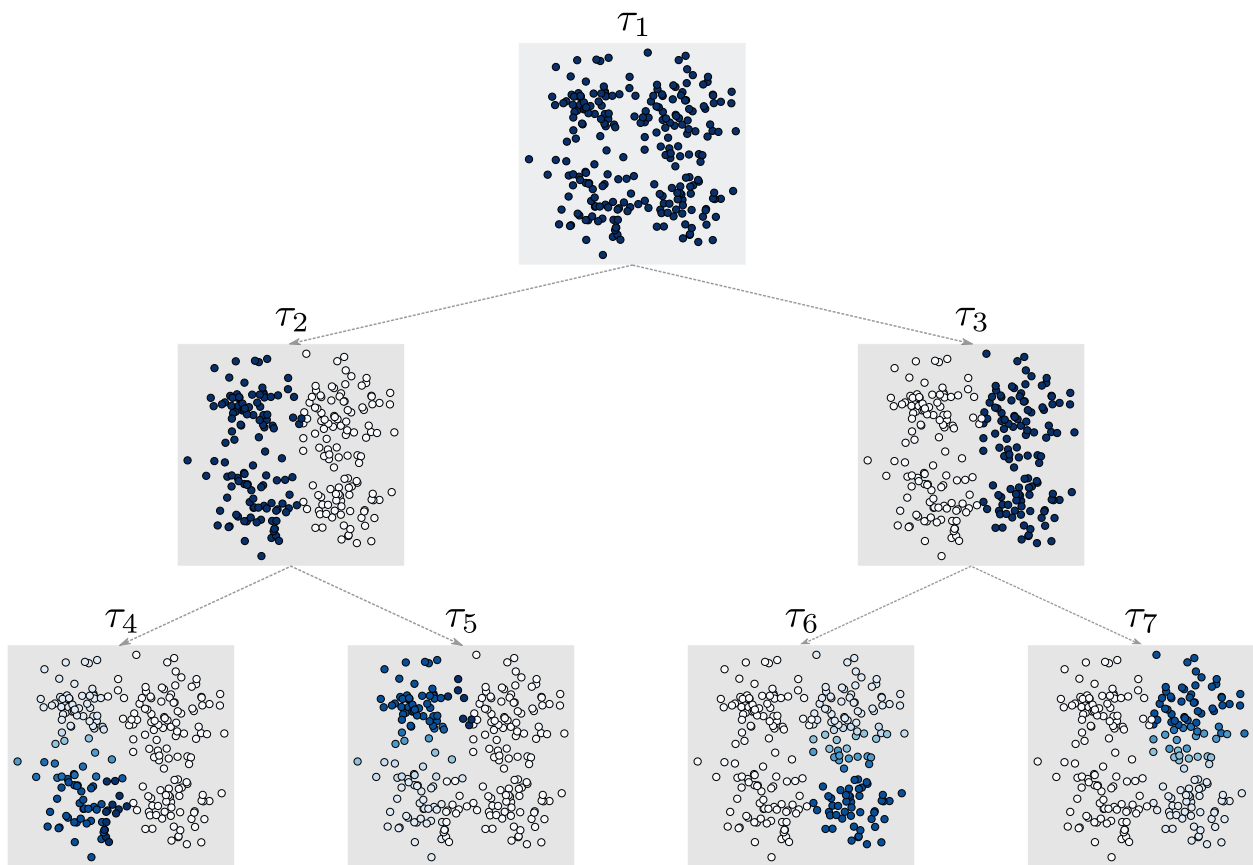


Figure 22: Output of the soft clustering post-process for a mixture of four Gaussians.

H Suggestions for setting the parameters

We discovered some rules of thumbs on how to set the various parameters. These are no formal results, just something we found to work well.

1. We run all our experiments considering all the cuts up to Ψ_{\max} . In practice we see that when we have reason to believe that there is a lot of noise in the cuts it is better to take only cuts up to 80th percentile of Ψ as this reduces the dependency on the quality of the cuts. Compare Supplement E.2, E.3 and F.4 for more details.
2. We set a between $1/3$ and $1/2$ of the smallest cluster that we want to find. See Supplements E.1 and F.2 for more details.
3. In the graph scenario, if we intend to use all the cuts we should pay attention to the fact that a enough cuts have good quality. To do so we need to set the lower bound in the FM algorithm quite close to the real proportion of the smallest cluster. This can be relaxed if we use less cuts by adjusting Ψ_{\max} . See Supplement F.3 for more details.